Accepted Manuscript

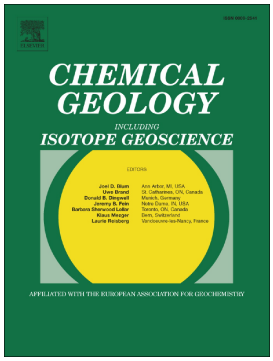

Coupling Δ47 and fluid inclusion thermometry on carbonate cements to precisely reconstruct the temperature, salinity and δ18O of paleo-groundwater in sedimentary basins

Xavier Mangenot, Magali Bonifacie, Marta Gasparrini, Alina Götz, Carine Chaduteau, Magali Ader, Virgile Rouchon

PII: S0009-2541(17)30566-1
DOI: doi:10.1016/j.chemgeo.2017.10.011
Reference: CHEMGE 18500

To appear in: *Chemical Geology*

Received date: 21 April 2017
Revised date: 5 October 2017
Accepted date: 7 October 2017

Please cite this article as: Xavier Mangenot, Magali Bonifacie, Marta Gasparrini, Alina Götz, Carine Chaduteau, Magali Ader, Virgile Rouchon , Coupling Δ47 and fluid inclusion thermometry on carbonate cements to precisely reconstruct the temperature, salinity and δ18O of paleo-groundwater in sedimentary basins. The address for the corresponding author was captured as affiliation for all authors. Please check if appropriate. Chemge(2017), doi:10.1016/j.chemgeo.2017.10.011

Coupling Δ_{47} and fluid inclusion thermometry on carbonate cements to precisely reconstruct the temperature, salinity and $\delta^{18}O$ of paleo-groundwater in sedimentary basins

Xavier Mangenot[1,2@], Magali Bonifacie[1], Marta Gasparrini[2], Alina Götz[2,3], Carine Chaduteau[1], Magali Ader[1], Virgile Rouchon[2]

[1] Institut de Physique du Globe de Paris, Sorbonne Paris Cité, Université Paris Diderot, UMR 7154 CNRS, 75005 Paris, France.
[2] IFP Energies nouvelles, 1-4 avenue de Bois-Préau, 92852 Rueil-Malmaison – France
[3] GeoZentrum Nordbayern, Universität Erlangen-Nürnberg, Schlossgarten 5, 91054 Erlangen, Germany
[@] xavier-mangenot@club.fr

HIGHLIGHTS

- Rock-based validation of the experimental Δ_{47} – T calibration for calcite and dolomite
- High-salinity fluids (from 0 to > 15 wt.% NaCl eq.) do not affect Δ_{47} signatures over crystallization of natural calcites and dolomites
- Rock-based validation of the absence of solid-state diffusion both for calcite and dolomite that experienced temperatures of 80°C for less than 50 Myr.
- Coupling FIM and Δ_{47} allows to evaluate if thermal and FI signatures were kept unaltered through geological times and to unravel temperature, $\delta^{18}O$ and salinity of paleo-groundwater

KEYWORDS. Fluid inclusions microthermometry; carbonate clumped isotopes; oxygen isotopes; salinity; $\delta^{18}O_{water}$

ABSTRACT

Diagenetic minerals may provide information about the burial history of geological units and can have practical applications, for instance, for reconstructing the geochemical and thermal histories of sedimentary basins. Clumped isotope, or Δ_{47}, thermometry on carbonates opens a new avenue for interpreting carbonate formation temperature and thermal history of rocks. Yet, most of current knowledge on Δ_{47} systematics has been acquired via theoretical or experimental studies with only limited validation by the rock-record at geological conditions/timescales. Here, we investigate calcitic and dolomitic cements representative of three genetically different cementation phases from a well-documented mineral paragenesis of a carbonate unit (Middle Jurassic, Paris basin, France). We compare Δ_{47} with fluid inclusions microthermometry (FIM) data that were independently obtained from the same calcite and dolomite crystal specimens. The range of homogenization temperatures (Th) found for Cal1, Cal2 and Dol1 fluid inclusions fit remarkably well (ie. within less than 5°C) with the temperatures determined from the Δ_{47} measurements (TΔ_{47}), for a temperature range between 60 and 100°C and salinities between 0 and 15 wt.% NaCl eq. This provides a consistent rock-based validation of the experimentally determined Δ_{47} calibration with formation temperature for both calcite and dolomite mineralogy. Such findings also confirm the applicability of Δ_{47} thermometry in low temperature diagenetic environments (ie., below circa. 100°C), which provides higher precision than FIM measurements (ie., typical uncertainties of ±

6°C with three Δ_{47} measurements) though significantly less time-consuming. Importantly, this study underlines how the coupling of both techniques can help to evaluate the degree of preservation of the original temperature information captured by either fluid inclusions or Δ_{47} compositions, and interpret each proxy as confidently/accurately as possible. Moreover, because both FIM and Δ_{47} measurements can provide independent constraints on the geochemistry of diagenetic paleofluids (via their salinity and $\delta^{18}O$ composition), this study also highlights the benefits of coupling both techniques to further unravel the nature of paleofuids. Finally, we propose a practical guideline as a basis for future applications of combined FIM and Δ_{47} thermometry.

1. INTRODUCTION

The temperature and chemical composition of diagenetic fluids are essential parameters for reconstructing the thermal and fluid circulation evolutions of sedimentary basins, allowing to reconstruct the detailed history of the porosity and permeability properties in reservoir rocks. Burial paleotemperatures of sedimentary successions are commonly inferred using various methods, including apatite fission-track and (U-Th)/He thermochronologies (Gleadow et al., 1986; Green et al., 2004), fluid-inclusions microthermometry (or FIM; e.g., Goldstein and Reynolds, 1994 and references therein) or the thermometry based on the isotopic equilibrium of oxygen between co-genetic minerals or between water and minerals (including carbonates) (e.g., O'Neil et al., 1969; Sharp and Kirschner, 1994). In the specific case of carbonate minerals, the most commonly used tools, namely FIM and $\delta^{18}O$ thermometry, are subject to several application limits potentially affecting the reliability (i.e., accuracy and precision) of the reconstructed mineralization temperatures. Notably, FIM, leading to both thermal and compositional information on the carbonate parent fluids, requires: (1) sufficiently clear and coarse crystals for accurate petrographic observations, (2) the occurrence of bi-phase fluid inclusions, large enough to be analyzed, (3) an evaluation of pressure correction to estimate true fluid trapping conditions (critical in over-pressured contexts; Vityk et al., 1994) and (4) that the inclusions have behaved as closed and isochoric systems through time. All the four previous requirements may not be satisfied, for a variety of reasons. Importantly, FIs in soft carbonate minerals may suffer different post-entrapment modifications (e.g. necking-down, stretching or leakage due to thermal reequilibration, refill processes; see Roedder and Bodnar 1980, Goldstein and Reynolds 1994 for an extensive review) that may induce erroneous evaluations of the conditions under which the FIs were trapped. On the other hand, the thermometry based on the exchanges of oxygen isotopes between water and carbonate can theoretically be applied to the entire range of diagenetic temperatures, but it requires independent knowledge of the oxygen isotopic composition of the formation fluids ($\delta^{18}O_{water}$). However, $\delta^{18}O_{water}$ of formation fluids can vary in time and space, due to a variety of factors, including mixing of fluids of different origins and/or the conditions of previous interactions with rocks (e.g., temperature, water/rock ratios).

The recently developed carbonate clumped isotope (or Δ_{47}) paleothermometry (Ghosh et al. 2006; Eiler, 2007) allows to independently access to both temperature and $\delta^{18}O_{water}$ values. The Δ_{47} thermometry is bind to an internal equilibrium inside the carbonate lattice where rare isotopes (^{13}C and ^{18}O) preferentially bond with each other as a function of temperature (Schauble et al., 2006). The relative abundance of $^{13}C^{18}O^{16}O_2$ groups in carbonate minerals depends on temperature (Schauble et al., 2006). In the last decade, the Δ_{47} thermometry has been calibrated in laboratory for a variety of inorganic and biogenic carbonates in the 0-350°C

geologically-relevant temperature range (e.g, Ghosh et al., 2006 ; Dennis and Schrag, 2010 ; Henkes et al., 2013; Bonifacie et al., 2017 ; Kele et al. 2015 ; Katz et al., 2017; Kelson et al., 2017). Laboratory experiments and theoretical studies have suggested that this tool is not influenced by the carbonate mineralogy or composition of the analyzed carbonate (e.g., Bonifacie et al., 2017), or by the precipitation conditions including the precipitation rate (e.g., Tang et al. 2014 ; Kelson et al., 2017; Watkins and Hunt, 2015), the pH and the salinity of the carbonate parent fluids (e.g., (Hill et al., 2014; Kluge and John, 2015). This suggests that the experimentally determined Δ_{47}–T calibrations could successfully unravel precise and accurate crystallization temperatures for a variety of natural carbonate precipitation conditions. Over the last decade, the Δ_{47} thermometry has thus been largely applied for reconstructing past temperatures of marine and continental carbonates precipitated at surface conditions (e.g., (Came et al., 2007; Huntington et al., 2010). Yet, the number of studies focusing on high-temperature settings remained limited (e.g, Bristow et al., 2011; Ferry et al., 2011; Loyd et al., 2012; Loyd et al. 2015; Dale et al., 2014; Henkes et al., 2014; Huntington and Lechler, 2015 ; Millan et al. 2016), likely resulting from the only recent availability of Δ_{47}–T calibrations for temperatures above 80°C (e.g., (Kluge et al., 2015) for calcite or (Bonifacie et al., 2017) for all carbonate minerals).

While Δ_{47} thermometry is applicable to the full range of temperature over which diagenetic carbonates can form, and presents unprecedented uncertainties (typically less than ± 3-4°C for T < 50°C, ± 6°C for T < 100°C and ± 8°C for T < 150°C; for more details see Figure 6c of Bonifacie et al., 2017 including both the precision on Δ_{47} data and the uncertainty on the Δ_{47}-T calibration), some complications about data interpretation may arise when studying carbonates that have been buried/heated over long durations (i.e., most pre-Quaternary carbonates). In this case, the initial abundance of ^{13}C–^{18}O bonds within the carbonate lattice (and thus the Δ_{47} value acquired at the time of precipitation) might have changed, even without dissolution/recrystallization of the carbonate phase, if temperature/time were high/long enough to have generated solid-state diffusion of atoms (e.g., Dennis and Schrag, 2010; Passey and Henkes, 2012 ; Bonifacie et al., 2013 ; Henkes et al., 2014; Stolper and Eiler, 2015). The reliability of the reconstructions of the original carbonate formation temperature could then be compromised. Experimental studies suggest that this process is limited to some "mild" burial conditions (e.g., calcite could start to lose its original Δ_{47} compositions only if at ~ 80-100°C for 100 Myr ; Passey and Henkes, 2012; Henkes et al., 2014; Stolper and Eiler, 2015). Three studies on metamorphic rocks or hydrothermal settings suggested that dolomite might be more resistant than calcite to this process (Bonifacie et al., 2013; Millan et al. 2016; Lloyd et al., 2017). Overall, most of the knowledge on potential resetting of Δ_{47} through solid-sate diffusion has been obtained on laboratory, short-scale, experiments on relatively simple, homogeneous and pure materials (eg., optical calcites; Passey and Henkes, 2012; Stolper and Eiler 2015) that might not capture the complexity of the natural realm. Also, a recent geological study suggested that solid-state diffusion may change original Δ_{47} values of both calcitic and dolomitic carbonates at milder diagenetic conditions than predicted by experimental studies (Winkelstern and Lohmann, 2016). Thus, before confidently upscaling laboratory experiments to geological samples, there is a need to investigate well-documented natural cases in order to gain more experience on conditions for resetting Δ_{47} values at geological timescales.

This contribution directly compares temperature estimates out of Δ_{47} ($T\Delta_{47}$) and FIM (Th) both carried out on the same cements (four calcites and one dolomite) hosted in the same carbonate unit (Middle Jurassic, Paris basin, France) characterized by a well-documented

paragenetic sequence. For the first time, we report here remarkably consistent Th and $T\Delta_{47}$ for both calcitic and dolomitic cements. This confirms the applicability of Δ_{47} thermometry in such geological conditions (60-100°C; salinity between 0 and 15 wt.% NaCl eq.), with higher precision than FIM measurements. Importantly, our finding also provides insight to highlight the benefits of coupling FIM and Δ_{47} measurements on the same samples for assessing the conservative nature of both proxies and/or further constraining the temperature, salinity and $\delta^{18}O$ of circulating paleofluids in sedimentary basins.

2. MATERIALS AND METHODS

2.1. Sample selection

This contribution focuses on the characterization of deep diagenetic fluids that have progressively cemented a Middle Jurassic carbonate reservoir unit (~ 165 Ma) from the Paris basin (Worden and Matray, 1995; Mangenot et al. in press). This subsurface carbonate unit has been widely studied as a potential exploration target for oil exploration, hydrological resource and CO_2 sequestration (Gaulier and Burrus, 1994). Our study investigates samples from two boreholes (*Baulne en Brie* and *Fossoy*), located in the center of the Basin, which were collected between 1600 and 1800 meters depth. The boreholes temperatures are currently about 60°C - 70°C (Ménétrier et al., 2005). Previous data on organic maturity and fluid inclusions thermometry consistently indicate that the maximum temperature reached higher values, between 80 and 100°C in the Late Cretaceous (Goncalves et al. 2010).

According to petrographic description and paragenetic relationships, the cementation history of the studied carbonate reservoir consists of three successive cementation episodes (Fig.1). From the oldest to the youngest: (1) a first blocky calcite cement, named Cal1 (crystal size of 100 µm-5mm), (2) a saddle dolomite cement, named Dol1 (crystal size of 500µm-2mm) and (3) a second blocky calcite cement, named Cal2 (crystal size of 100-1mm). Petrographic features of each of these diagenetic pore-filling cements are illustrated in figure 1. The Cal1, Cal2 and Dol1 cements display very distinctive cathodoluminescence patterns (Fig. 1) suggesting different formation conditions (e.g. fluid redox, Mn and Fe concentrations; Machel, 1985). The Δ_{47} and FIM thermometers were conjointly applied for comparison on five cement specimens of Cal1, Cal2 and Dol1.

2.2 Fluid inclusion micro-thermometry (FIM)

Five double-polished thick sections were prepared with a cold technique to prevent re-equilibration of the fluid inclusions (FIs) (McNeil and Morris, 1992). The petrographic selection of suitable fluid inclusions allowed microthermometry measurements on five different samples out of Cal1 (n=2), Cal2 (n=2) and Dol1 (n=1) cementation episodes. The rock-slabs used for thick-section preparation were selected to include the same sub-samples than those drilled for recovering powder for clumped isotope measurements. Primary inclusions, trapped during mineral growth were carefully differentiated from few secondary inclusions, trapped along healed micro-fractures, formed after cement growth. Prior to microthermometric measurements, petrographic observations were done to distinguish consistent fluid inclusion assemblages (FIA) and characterize FI size, shape, occurrence and the proportion of liquid *versus* gas phases (as suggested by Goldstein and Reynolds, 1994). FI microthermometry was performed with a Linkam MDS 600 heating–freezing stage, mounted on a Nikon LV100 Eclipse microscope, associated to a 100W Mercury vapor lamp. The

Linksys 32 software enabled all the operations for FI microthermometry. The stage was calibrated with synthetic fluid inclusions in quartz standards on the following temperatures: ice (H_2O) melting point at 0.1 °C, eutectic point of a NaCl-H_2O brine at -20.9 °C and a chemical standard (Hack 11/87) melting point at 135 °C. The measurements of homogenization temperatures (Th) were carried out before freezing runs to avoid stretching of the inclusions by ice nucleation. The accuracy of the microthermometry data are about ± 1 °C for heating runs and about ± 0.5 °C for cooling runs. Beside Th and final melting temperatures of ice (Tm_i), further observations allowed to determine the temperatures of gas nucleation after homogenization (Tn_g) and the temperatures of ice-like phases nucleation (Tn_i) during freezing, these permitting to ascertain the common behavior of FIs from the same generation. The apparent eutectic temperature (Te_{ap}), recorded during FI reheating after freezing. is the temperature at which the first liquid is observed and overestimates true eutectic temperatures. Furthermore, when the final melting occurred abruptly (metastable behavior), possibly at temperatures above the real melting, a Tm_{MET} was reported. The software package FLUIDS (Bakker, 2009, 2003) was used to further characterize the aqueous fluids. AQSO1 was used to calculate total salinities from measured Tm_i in the binary H_2O–NaCl system (Bodnar, 1993). The application BULK was employed to calculate bulk fluid properties (e.g. density) of individual FIs using the equation of state of Krumgalz et al. (1996) and the measured Th and Tm_i. The program LONER32 was used to calculate isochore slopes, according to the thermodynamic model of Bodnar and Vityk (1994) by inputting measured Th and salinities (expressed as wt. % NaCl eq.).

2.3. Δ_{47}, $\delta^{18}O$ and $\delta^{13}C$ measurements and data processing

The required amount of carbonate for 3 replicate Δ_{47} measurements (ie. ~15-20 mg) was collected with a dental drill from the same slabs used for thin and thick sections preparation. Based on transmitted light and CL microscopic observations, petrographically homogenous crystals were screened and selected to prevent mixing of different phases. A total of ten Cal1 cements, two Cal2 cements and one Dol1 cement were selected and measured for their respective Δ_{47} composition. Among all the 13 cement samples characterized here for their Δ_{47} value, five were chosen (based on petrographic criteria) for direct comparison of temperatures obtained with Δ_{47} and FIM measurements. The selected sample specimens (BEBJ8, BEBJ12, BEBJ2, BEBJgeode and FOS1610) are representative of their respective populations in terms of petrographic texture, cathodoluminescence response and traditional isotopic compositions (i.e. very homogeneous $\delta^{18}O_{carb}$ and $\delta^{13}C_{carb}$ inside each investigated generation).

Measurements of Δ_{47} composition of carbonate samples were performed at *Institut de Physique du Globe de Paris* (IPGP, stable isotopes team) using a Thermo Scientific MAT 253 gas-source mass spectrometer. Isotopic measurements were performed on gaseous CO_2 released after digestion of carbonate powder in 104% phosphoric acid. About 5-8 mg of carbonate samples were reacted at 90°C in a common acid bath for 20 minutes for calcites and 1 hour for dolomites. Note that recent analytical development allows reaching good precision on $T\Delta_{47}$ with only 1-2 mg of carbonate powder in total (Müller et al., 2017). The methods used for carbonate digestion, CO_2 purification, mass spectrometric measurements and a posteriori data processing follow the procedure detailed in Bonifacie et al. (2017) and is only briefly summarized below.

Each measurement consisted of seventy cycles of comparison between the CO_2 extracted from sample against a working internal reference CO_2 gas provided by Oztech Trading Corporation (with $\delta^{13}C_{VPDB}$ = - 3.72‰ and $\delta^{18}O_{VPDB}$ = - 6.06‰, verified with international

carbonate reference material NBS19). The signal integration time was of 26 seconds by cycle (i.e., total integration time of 1820 seconds for each CO_2 sample) for a signal of 12 or 16V on m/z = 44.

Traditional $\delta^{18}O$ and $\delta^{13}C$ data were acquired as part of each Δ_{47} analysis and ^{17}O corrections were made using the ^{17}O parameters from Santrock et al. (1985), as for the majority of Δ_{47} data and calibrations published to date. Note that using the ^{17}O parameters from Brand et al. (2010) would only lead to small differences in Δ_{47} values of both of our standards and samples (ie. less than ±0.010‰), well within the analytical uncertainty on Δ_{47} measurements. This would thus not significantly change the reported temperatures (and conclusions) of this study. In order to account for the temperature dependence of oxygen isotope fractionation between CO_2 gas and carbonate resulting from the reaction with phosphoric acid at 90°C, fractionation factors of 1.00811 and 1.0093 were respectively used for calcite and dolomite (following Rosenbaum and Sheppard (1986) and Katz et al. (2017)). $\delta^{18}O$ and $\delta^{13}C$ of the carbonate samples are expressed in per mil with respect to the VPDB standard.

In order to be able to report our Δ_{47} data in the absolute reference frame, we measured CO_2 gases driven to isotopologue equilibrium at 1000 and 25°C (typically one of these two type of gaseous CO_2 standards was analyzed every day and every 4-5 analyses), along with the samples in order to check for analytical stability. These equilibrated CO_2 gas standards have bulk isotopic compositions spanning the entire range of measured cement samples, are purified and analyzed in the same way as carbonate samples or carbonate standards and are typically run every 4-5 analyses (Table S1). The raw Δ_{47} data were first corrected for linearity effects using a fixed common Equilibrated Gas Line slope fitted to the equilibrated CO_2 gases at both 1000 and 25°C. Subsequently, as recommended by Dennis et al., (2011), the raw Δ_{47} values (expressed relative to the working gas) were transferred into the Carbon Dioxide Equilibrated Scale (CDES) using the CO_2 gases driven to isotopologue equilibrium both at 1000 and 25°C with theoretically predicted Δ_{47} values of 0.0266‰ and 0.9252‰, respectively (after Wang et al., 2004). Finally, $\Delta_{47CDES90}$ data were projected into the 25 °C acid digestion reference frame ($\Delta_{47CDES25}$ in Table 2) for easier comparison with previously published calibration data. For this, we added the acid fractionation value of + 0.092‰ determined by Henkes et al. (2013) and confirmed at IPGP. All the Δ_{47} data of the present study were obtained in six distinct sessions of analyses performed over a period of one year, each separated by several weeks. The duration of each session was typically 2–5 weeks, corresponding to about 10–23 equilibrated CO_2 gases used for constructing the CDES correction frames. All the isotopic values of equilibrated CO_2 standards can be found in Table S1 together with values of samples and carbonate standards.

To guarantee accuracy of the Δ_{47} data, we routinely analyzed two carbonate reference materials (IPGP-Carrara marble and 102-GCAZ01b, also reported by Dennis et al., 2011 and many other studies). One of these two carbonate standards was analyzed typically every five analyses and distributed along the diagenetic cement samples in all runs in order to check for analytical stability/accuracy of the whole procedure (including carbonate digestion, CO_2 purification, stability of the conditions for analyses of CO_2 inside the mass spectrometer and/or accuracy of the correction frames constructed with standards of equilibrated CO_2 gas – namely the accuracy of the equilibrated gas lines and empirical transfer function lines), as well as long-term external reproducibility of our Δ_{47} measurements. The Δ_{47} values obtained for these carbonates over the course of this study (July 2014-May 2015) are: $\Delta_{47CDES25}$ =

0.412 ± 0.016‰ (1SD, n=28) for IPGP-Carrara; $\Delta_{47CDES25}$ = 0.721 ± 0.020‰ (1SD, n=21) for 102-GC-AZ01b. Those $\Delta_{47CDES25}$ values are indistinguishable from these obtained in other laboratories (e.g. Dennis et al. 2011; Henkes et al. 2013) and on a longer timescale at IPGP (Bonifacie et al. 2017; Katz et al., 2017). The internal one standard error uncertainty of each Δ_{47} measurement is close to the shot noise limit (that is ± 0.009‰ in our analytical conditions). The external reproducibility, that is the standard deviation of replicate analyses of the same sample, is usually larger and is reported in Table 2. The final Δ_{47} uncertainty reported for samples is the standard error of the mean (S.E.) calculated as the standard deviation (S.D) of all carbonate standards replicates (±0.018‰ in this study ; n=49) divided by the square root of the number of sample replicates. When S.D. of the sample was higher than 0.018‰, S.E. was calculated as S.D. of the sample replicates, divided by the square root of the number of sample replicates.

Finally, the corrected Δ_{47} values were converted into temperatures using the composite Δ_{47}-T calibration determined for all carbonate minerals for the 0-300°C temperature range (ie., Equation (3) from Bonifacie et al. 2017 that compiles 103 mean Δ_{47} data from seven different laboratories and with proper error propagation, which is $\Delta_{47CDES25} = 0.0422*10^6/T + 0.2182$ in the 25°C acid digestion frame). The oxygen isotopic compositions of the water ($\delta^{18}O_{water}$) from which the carbonates precipitated were calculated for each estimated $T\Delta_{47}$ using the $\delta^{18}O_{carb}$ values measured for the carbonate as well as the oxygen isotope fractionation between the carbonate and water from O'Neil et al. (1969) for calcite and (Horita, 2014) for dolomite.

2.4. $\delta^{18}O$ and $\delta^{13}C$ profiles in samples BEBJ8

In order to evaluate the heterogeneity of the analyzed cements, we also performed a $\delta^{13}C_{carb}$ and $\delta^{18}O_{carb}$ analyses through different sub-zones of a single specimen of about 2 cm in length (sample BEBJ8 from Cal1 cement) by drilling 3-4 mg of powder every 250µm. About 1-2 mg of the carbonate powders were reacted with 100% phosphoric acid at 70°C using a Gasbench II connected to a ThermoFisher Delta V Plus mass spectrometer (Nürnberg university). All values are reported in per mil relative to V-PDB. Reproducibility and accuracy was monitored by replicate analysis of laboratory standards calibrated by assigning $\delta^{13}C$ values of +1.95‰ to NBS19 and -46.6‰ to LSVEC and $\delta^{18}O$ values of -2.20‰ to NBS19 and -23.2‰ to NBS18. External reproducibility for $\delta^{13}C$ and $\delta^{18}O$ was ±0.02‰ and ±0.01‰ (1 SD), respectively.

3- RESULTS

3.1. Fluid-inclusions (FIs) petrography

Table 1 and figure 3 summarize the main petrographic features and the microthermometry results for the studied FIs in Cal1, Cal2 and Dol1. Different FIA were established based on the FI location within the crystals (e.g. crystal core, growth zones, patches etc.).

In Cal1 cements, about half of the FIs are mono-phase (c.f. Fig.3.F) at room temperature (20 °C), and are thus inappropriate for microthermometric measurements. These cements also contain bi-phase liquid-rich FIs (containing a vapor bubble and a colorless liquid; Fig.3D), that are useful for Th and Tm_i measurements. The bi-phase FIs are mostly concentrated in patches, along growth zones or cleavage planes and less commonly they occur isolated or

aligned along pseudo-secondary trails. They display consistent sizes (3-12µm) and variable shape, often controlled by crystallographic planes and less commonly irregular or oblate. Except for some leaked inclusions, the volume fraction of the liquid phase at room temperature is relatively constant with a degree of fill (F) varying between 0.94 and 0.98.

The investigated Cal2 cements contain mono-phase liquid FIs and most bi-phase liquid-rich FIs. They occur isolated, in patches or along cleavage planes with both consistent sizes (3-8µm) and volume fraction of the liquid phase (0.95-0.98). The FIs shape is dominantly irregular, controlled by crystallographic planes or oblate.

Fluid inclusions in Dol1 crystals are densely distributed in three dimensions and are mainly concentrated in the crystal cores (Fig. 3.A.C), pointing to a primary origin. These inclusions are up to 5 µm in length and have an irregular shape, which may mimic the crystallographic directions of the host crystal. Inclusions are dominantly bi-phase liquid-rich, with a consistent liquid volume fraction (F) between 0.90 and 0.96.

All the observed FIs (mono- and bi-phase) in Cal1, Cal2 and Dol1 crystals contain an aqueous fluid, as suggested by the lack of fluorescence when observed under UV-light. A total of 151 bi-phase inclusions (n=56 for Cal1, n=63 for Cal2 and n=31 for Dol1), within suitable petrographic assemblages (FIA), were assigned a primary origin and thus considered for microthermometry analyses.

3.2. Fluid-inclusions microthermometry

The analyzed bi-phase FIs in Cal 1, Cal2 and Dol1 present a narrow range of degree of fill (F), suggesting homogeneous trapping of the diagenetic fluids at the time of carbonate precipitation. Total homogenization occurred in the liquid phase for all inclusion types. During the first cooling run after homogenization, the vapor bubble was metastably absent at room temperature and did not renucleate, indicating a significant amount of metastability. The nucleation of a vapor bubble was observed in some of Cal1 and Cal2 FIs after cooling them to 0 or -3 °C for several hours. In other cases, the vapor bubble nucleated only after the cooling runs and consequent freezing of the liquid phase, during re-heating. The studied FIs froze during the first cooling run mainly at temperatures between -50 and -70 °C. During reheating a first melting (Te_{ap}) could be observed only for few FIs at temperatures between -10 and -25 °C, rather suggesting a fluid system dominated by NaCl. The last solid phase to melt was possibly ice (roundish and whitish crystals). The final melting of ice occurred with a stable (gradual melting of the ice crystals; Tm_i) or metastable (Tm_{MET} ; abrupt melting of the ice crystals) behavior.

FIs analyzed in Cal1 (BEBJ12 and BEBJ8 samples) homogenized in the range 45-91°C, though most Th fall in the range 50-70 °C (c.f. Fig.4. A. B; Table 1). The frequency histograms for Th data show a normal Gaussian distribution for BEBJ8 with a well-defined mode at 55-65°C (BEBJ8) and a flatter distribution for BEBJ12 with a poorly defined mode at 65-70°C . The Tm_i data recorded in Cal1 range from -10.1 to -12.8°C (with a pronounced mode at -11°C), corresponding to salinities between 8.4 and 18.8 wt.% NaCl eq. (mode at 14%) up to salinities 5 times higher than normal seawater. FIs in Cal2 (BEBJ2 and BEBgeode samples) homogenized in the range 60-100 °C, though most Th fall in the range 65-90 °C (c.f. Fig.4. C, D; Table 1). The frequency histogram for Th data shows a normal Gaussian distribution with well-defined modes at 75-85 °C (BEBJ2) and 65-80 °C (BEBgeode). The Tm_i measured in Cal2 FIs show a large spread (from -0,1 to -9 °C), corresponding to salinities

of 0.2-12.8% wt.% NaCl eq., covering a wide spectrum of fluids which go from a concentrated brine to a freshwater endmember. FIs in Dol1 crystals display Th data falling in the range 70-110°C with normal Gaussian distribution and a well-defined mode value at 90-95°C (Fig. 4. E; Table 1). Dol1 FIs show Tm_i in a narrow range (-6.7 to -7.8 °C), corresponding to salinities well clustered around 10.5 wt.% NaCl eq.

The overall microthermometry dataset obtained for Cal1, Cal2 and Dol1 matches with the definition of a consistent FI dataset (Goldstein and Reynolds 1994) since more than 90% of the Th data, within individual FIA, fall in a range of ±10°C. The fact that FIs with variable size and shape in Cal1, Cal2 or Dol1 record consistent degree of fill (F) and a narrow range of Th variation within individual FIA, attests that they did not experience significant post-entrapment modifications (e.g. necking-down, stretching or leakage due to thermal reequilibration), possibly remaining a closed and isochoric system. Only minor thermal reequilibration may be suspected to have occurred in the few Cal1 FIs recording Th above 70 °C (Fig. 4A, B). Consequently, the investigated FIs may be considered to have preserved precious information on the original temperature and salinity of the fluids responsible for the three successive episodes of carbonate cementation. Thus, the thermal and compositional information issued from the five selected cements is appropriate to be compared with the information derived from clumped isotope (Δ_{47}) analyses out of the same mineral specimens which thus represent excellent targets for the planned analytical comparison.

3.3. FI pressure correction

Homogenization temperatures (Th) obtained by FIM measurements correspond to the minimum trapping temperatures (Tt) of the fluids (Goldstein and Reynolds, 1994). A geologically coherent pressure correction (Pc) has to be applied to Th in order to obtain more accurate estimations of the true entrapment temperatures (Roedder and Bodnar, 1980), which for primary FIs, also correspond to the crystal growth temperatures.

Such pressure correction requires to set constraints on both the fluid density (calculated as a function of the mode salinity values, measured for each carbonate phase; c.f. Table 1) and the trapping pressure, in the assumption that FIs have behaved as a closed and isochoric system. However, the fluid trapping pressure (Pt) is most often unknown and has to be inferred indirectly (Roedder and Bodnar, 1980). The Middle Jurassic reservoirs of the Paris basin are currently governed by hydrostatic pressure conditions (10MPa/km; Goncalves et al., 2010) and are considered not to have experienced any major overpressure during their geological evolution (c.f. basin modeling of Gonçalvès et al., 2010). Hence, we inferred trapping pressures of 16, 22.5 and 27.5 MPa for Cal1, Cal2 and Dol2 parent fluids, respectively. This calculation was based on a geothermal gradient of 30°C/km (Gaulier and Burrus, 1994) which was likely characteristic of the Paris basin during its Mesozoic evolution, a mean surface temperature of 20±5 °C, a hydrostatic geobarometric gradient of 10MPa/km and the mean Th values measured in FIs from Cal, Cal2 and Dol1 crystals. Such pressure conditions allow to correct the mean Th values and to estimate possible trapping temperatures (Tt) of 70°C, 88°C and 102°C for FIs in Cal1, Cal2 and Dol1, respectively. Pressure corrections calculated by using minimum (15°C) and maximum (25°C) surface temperatures would induce only a minor variation (1 to 2°C) in the calculated Tt (Fig. 5).

3.4. Isotope results (Δ_{47}, $\delta^{18}O_{carb}$, $\delta^{13}C_{carb}$, $\delta^{18}O_{water}$)

Table 2 summarizes the stable isotopic data ($\delta^{18}O_{carb}$, $\delta^{13}C_{carb}$, Δ_{47}) for the three generations

of calcite and dolomite cements, together with their respective $T\Delta_{47}$ and $\delta^{18}O_{water}$ derived from this dataset. Detailed information on the raw Δ_{47} data and post-acquisition corrections and standardization can be found online in Supplementary Appendix 1. The three generations of carbonate cements show distinct oxygen isotopic compositions that are respectively averaging at $\delta^{18}O_{carb}$ = -6.41 ± 0.68‰ (1S.D., n=10 samples) for Cal1, $\delta^{18}O_{carb}$ = -15.26 ± 0.08‰ (1S.D., n=2 samples) for Cal2 and $\delta^{18}O_{carb}$ = -9.57‰ for Dol1 (n=1) (Fig.7). Within each cement population, the $\delta^{18}O_{carb}$ values are showing only limited variation, also supported at smaller scale for the Cal1 population with the BEBJ8 sample, for which sub-zones (2-4 mg) were drilled along a 2cm length cement (Fig.6). This cement displays constant isotopic compositions averaging $\delta^{18}O_{carb}$ = -7.28 ± 0.32‰ and $\delta^{13}C_{carb}$ = 1.24 ± 0.26‰ (1 S.D., n=7; Fig. 6). The Δ_{47} values found for Cal1, Cal2 and Dol1 are respectively clustered at 0.588 ± 0.004‰ (S.E, n=24 analyses), 0.550 ± 0.008‰ (S.E, n=5 analyses) and 0.524 ± 0.010‰ (n=3 analyses), which translates in very homogeneous average $T\Delta_{47}$ temperatures for each cement population of 65±3°C, 84±4°C and 98±7°C, respectively (c.f. Fig7). For each investigated population, the calculated average $\delta^{18}O_{water}$ values is about +3‰ for Cal1, -3‰ for Cal2, and +1‰ for Dol1. Overall, these results suggest that Cal1, Cal2 and Dol1 cements have precipitated at three distinct temperatures and from distinct paleofluids.

4- DISCUSSION

4.1. Comparison of mineral growth temperature estimates out of FIM and Δ_{47} data

The Δ_{47} temperatures ($T\Delta_{47}$) found for Cal1, Cal2 and Dol1 cements fit remarkably well (ie. within less than 5°C) with the range of homogenization temperatures (Th) measured from FIs within the same samples (Fig. 4). Indeed, in the 60-100°C temperature range, the Th and $T\Delta_{47}$ obtained in this study on both calcitic and dolomitic phases are strongly correlated and are unresolvable from the 1:1 line in Figure 8. Consistency remains when pressure-corrected Th (Tt) are considered. The excellent match between Th and $T\Delta_{47}$ suggests that both FIs and Δ_{47} composition record thermal conditions of carbonate precipitation for each phase of cementation investigated (Cal1, Cal2, Dol1) and were likely not altered since the time of mineral growth (ie., absence of ^{13}C–^{18}O bond reordering via solid state diffusion and absence of FI stretching and/or leakage due to thermal reequilibration, necking-down, refill processes, etc). Such hypothesis finds support in: 1/ current knowledge on the temperature–time conditions needed to change Δ_{47} of calcites and dolomites via solid-state diffusion (e.g., (Dennis and Schrag, 2010; Bonifacie et al., 2013; Henkes et al., 2014; Lloyd et al., 2017; Stolper and Eiler, 2015), that are well above the conditions experienced by our studied carbonate unit, as independently determined by Ménétrier et al., (2005), Garibaldi, (2010) and Goncalves et al. (2010); and 2/ the petrographic characteristics of the FIs chosen for microthermometry as well as the dominantly gaussian distribution of measured Th (Fig 4). Indeed, if any FI post-genetic alteration had occurred, like thermal reequilibration, this could not have affected all FIs equally – as the FI resistance depends on their host mineral, size, shape, proximity to cleavage planes, etc – and would have led to an asymmetric distribution of Th (Goldstein and Reynolds, 1994; Tobin and Claxton, 2000). Importantly, the cross-consistent $T\Delta_{47}$ and Th data obtained here strongly suggests that the measured Δ_{47} values of the carbonate were acquired at the time of its precipitation, and conjointly with the oxygen isotopic composition of the carbonate $\delta^{18}O_{carb}$. Then, the $\delta^{18}O_{water}$ of the mineralizing fluid can be confidently calculated using the $T\Delta_{47}$ and $\delta^{18}O_{carb}$ values measured for the carbonate as well as the oxygen isotope fractionation factor between the carbonate and water (see the methods section for more details).

More broadly, this first FIM and Δ_{47} cross-consistent temperature dataset has two main consequences for the validity of the Δ_{47} thermometry for studying natural samples in burial diagenetic conditions. Based on the number of replicates analyzed, this study provides a natural rock-based validation of: 1/ the inter-laboratory Δ_{47} –T calibration recently published for all carbonate minerals, including calcite and dolomite (Bonifacie et al., 2017), and 2/ the fact that high-salinity fluids (from 0 to > 15 wt.% NaCl eq.) do not affect Δ_{47} signatures over crystallization of natural calcite and dolomite, in agreement with the experimental data of Kluge and John (2015).

Some recent studies have also compared temperature estimates out of Δ_{47} and FIM measurements on dolomite samples (Came et al., 2016; Macdonald et al., 2017; Millán et al., 2016). It is noticeable that while carbonates we investigated here are strongly correlated and unresolvable from the 1:1 line, the previously reported data are all showing significant offsets from this 1:1 line, as well as more scattered relationships between Th and TΔ_{47} (Figure 8). In detail, although the ten dolomitic samples from Came et al. (2016) are distributed both above and below the 1:1 line, they show only very weak correlation between Th and TΔ_{47}. To explain this weak relationship between their TΔ_{47} and Th, Came et al. (2016) mentioned possible imprints of the solid-state diffusion for some of their samples. Indeed, their samples were heated up to 120°C during 300 Ma and up to 160°C at the peak of burial (Williams et al., 1998), conditions that may have induced solid-state diffusion. Based on petrographic observations, they ruled out thermal re-equilibration of their FI assemblages during burial. On the other hand, for the seven dolomites studied in Macdonald et al. 2017, Th and TΔ_{47} are slightly correlated, but Th are significantly higher than TΔ_{47} (by about ~ 20-60°C) (i.e., blue circles are all on the right side of the 1:1 line in Fig. 8). These authors suggested that their TΔ_{47} are conservative of the original crystallization conditions over burial, whereas their Th would reflect recent resetting at the borehole ambient temperatures (also supported by the ~ 60°C spread of Th recorded in each single cement specimen). Though it is noticeable that in these previous studies, published Th values were likely not corrected for pressure effects (which would increase temperatures deduced from FIM), and published TΔ_{47} were calculated with Δ_{47}–T calibration equations that are different to the one used here, determining the reasons of such differences between their TΔ_{47} and Th are beyond the scope of our study. Note however that the TΔ_{47} from Millan et al. 2016 were calculated with the calibration from Kele et al. (2015) that is statistically indistinguishable from the one used here, and thus that the fact that their TΔ_{47} are 10-20°C higher than their Th is likely due to the lack of pressure correction of the fluid inclusion measurements.

Alternatively, we emphasize in the following that when both Δ_{47} values and FI assemblages are not changed since the time of carbonate crystallization (which can be shown by consistent TΔ_{47} and Tt estimates as in our study), FIM and Δ_{47} measurements allow to faithfully record a snapshot of the composition of the mineralizing fluid, including its salinity and oxygen isotopic composition ($\delta^{18}O_{water}$). Section 4.3 further illustrates various information on temperature (including peak burial temperatures and paleo-pressure of carbonate precipitation) and composition of mineralizing fluids that can be obtained when coupling FIM and Δ_{47} measurements, including when TΔ_{47} and Th are not matching.

4.2. Characterization of $\delta^{18}O_{water}$ and salinities of mineralizing fluids

The salinity and the $\delta^{18}O_{water}$ values of diagenetic fluids can help constraining their origin and revealing the hydrogeological and basin evolution histories. We here use our results on the

three different generations of cements (Cal1, Cal2 and Dol1) to illustrate the potential of the paired application of FIM and Δ_{47} measurements to reveal information about paleofluid circulations. Note that a discussion of the geological significance of such observations at the basin scale is beyond the scope of this study and are undertaken elsewhere (Mangenot et al. in press).

In the case of the Cal 1 generation, the independently obtained $T\Delta_{47}$ and $\delta^{18}O_{carb}$ values allow to calculate a $\delta^{18}O_{water}$ of the mineralizing fluid that is enriched in ^{18}O compared to global modern seawater ($\delta^{18}O_{water}$ = 0‰), with average $\delta^{18}O_{water}$ of 3.1‰. In parallel, FIM measurements reveal a salinity mode at 14 wt.% NaCl eq., also higher relative to modern seawater (3.5 wt% NaCl eq.). Both enrichment in ^{18}O and salinities relative to seawater suggest a mineralizing fluid with an evaporative origin. Such compositions are comparable with those measured in porewaters from the underlying Triassic formation, with salinity up to 20% and $\delta^{18}O_{water}$ up to 2.5‰ (Worden et al. 1999). The evaporate origin of this water also agrees with others independent geochemical data (e.g. Cl/Br, Li contents; Matray et al. 1995). Importantly, this Triassic reservoir was suggested to be the source of an upward cross-formational flows occurring between the Middle Jurassic and Triassic aquifers (Worden et al. 1995; Mangenot et al. in press).The fact that modern Triassic waters are more enriched in salt and more depleted in ^{18}O compared to Cal1 fluids likely results from recent meteoric water infiltration. This water would have dissolved evaporite deposits and enriched the alkaline components, associated with a depletion in ^{18}O because of the meteoric origin of the water (this is discussed in detail by Worden et al. 1999).

For the Cal 2 generation, the calculated $\delta^{18}O_{water}$ and the measured salinities are also showing compatible information regarding the origin and evolution of the parent fluids. Indeed, the Cal2 paleowaters display average $\delta^{18}O_{water}$ = – 3.4‰, suggesting a meteoric freshwater origin. Such water isotopic composition seems consistent with Cal2 fluid inclusion salinities, suggesting a fluid evolution from a brine end-member towards a freshwater endmember (eleven fluid inclusions ranging from 12.8 to 0.2 wt.% NaCl eq.). Such water geochemistry reconstructed from diagenetic cements is consistent with the present-day $\delta^{18}O_{water}$ and salinity of formation waters within aquifers hosted in Middle Jurassic lithologies (with $\delta^{18}O_{water}$ between -3 and -6‰ and TDS of 0.2-3.5%; (Matray et al., 1994).

For the Dol1 generation, more complex hypotheses on the origin and evolution of the parent fluids are needed to reconcile the calculated $\delta^{18}O_{water}$ and measured salinities. Indeed, the Dol1 cements have precipitated from a fluid with $\delta^{18}O_{water}$ of circa 0.9‰ (close to normal modern seawater values) while FI salinities are from 10.1 to 11.5% wt.% NaCl eq. (which is three times higher than seawater). Such a combination of paleofluids compositions could be explained by two distinct scenarios: (1) an initial marine fluid, enriched in salt by water-rock interaction and dissolution of evaporitic rocks (e.g. halite) which did not buffer the fluid oxygen isotopic composition or (2) trapping of an initial highly saline brine from an evaporative context that would then be diluted by meteoric waters until reaching a $\delta^{18}O_{water}$ close to marine values and intermediate salinity values.

These cases underline the strength of coupling Δ_{47}–FIM on the same samples for reaching more complete and/or accurate reconstruction of the diagenetic history, since the complexity of the origin and evolution of the fluid recorded might not have been as clearly/confidently decoded if only one of the two methods was applied – see more details in section 4.3 (case 1).

4.3. Benefits of coupling FIM and Δ_{47} measurements

This section presents different possible scenarios that can be observed when combining Δ_{47} and FIM measurements on the same carbonate specimens. It also underlines that, in some cases, the combination of Δ_{47} and FIM measurements can help putting further constraints on the peak burial temperatures experienced by the host-rocks or the pressure at which carbonates precipitated.

The susceptibility of post-genetic alteration of the primary Δ_{47} and FI signals is critical for the confident reconstruction of the mineral paragenesis and thermal history of the investigated rocks and, at a larger scale, the sedimentary basins. However, as discussed above thermal resetting might, in some conditions, obscure the primary signal of either Δ_{47} and/or FIM and lead to false interpretations (even if kept as a closed system). As both thermometers can be reset *internally* in the absence of recrystallization such resetting might be particularly challenging to detect, notably because the degree to which the original signature is changed depends on several factors. Known controls over FI stretching or leakage (due to thermal reequilibration processes) include the softness of the host mineral, the size and shape of the FIs, their proximity to lattice imperfections or crystallographic orientations, the strain rate and heating duration, the fluid composition and the amount of overheating and confining pressure (Tobin and Claxton, 2000 and references therein). On the other hand, previous studies suggest that the susceptibility or rates of ^{13}C-^{18}O bonds reordering include temperature and heating/cooling duration (e.g., Dennis and Schrag, 2010; Henkes et al., 2014; Passey and Henkes, 2012), mineralogy (e.g., Bonifacie et al., 2013; Lloyd et al., 2017), crystal coarseness (e.g., Siman-Tov et al., 2016; Winkelstern and Lohmann, 2016) and/or optical properties (e.g., Shenton et al., 2015). We underline here the importance of coupling FIM and Δ_{47} measurements to detect such resetting processes, and to reconstruct temperature, salinities and $\delta^{18}O$ compositions of the mineralizing fluids in the most confident way.

Figure 9 illustrates four hypothetical burial scenarios that can be found in natural/geological conditions, and summarizes the kind of information that can be obtained from coupling Δ_{47} and FIM measurements. Importantly, Figure 9 only describes cases for which neither dissolution/recrystallization nor petrographic changes have occurred in the host-carbonate (e.g., no change of $\delta^{18}O$, $\delta^{13}C$ or elemental compositions since the time of precipitation), together with no change on FI chemistry (assuming that no refill processes have occurred). We however acknowledge that other/more complex cases are possible in nature, and recommend the authors of future applied studies to consider independent geological information to comfort their interpretations when possible.

Case 1 (Fig. 9) describes a situation where trapping temperatures (Tt) match $T\Delta_{47}$ values, likely due to the absence of thermal resetting of both initial FIM and Δ_{47} signatures since the original carbonate crystallization. In such case, Δ_{47} and FIM measurements allow to have direct access to important information on the temperature and the composition of the mineralizing fluid: its salinity (that is directly measured) and its oxygen isotopic composition $\delta^{18}O_{water}$ (that is precisely estimated from $\delta^{18}O_{carb}$ and $T\Delta_{47}$). This case is illustrated by the Paris basin investigated here with examples of the revealed information presented above (Section 4.2).

It is noteworthy that for our case study, FI thermometry displays systematically higher uncertainties on temperature estimates (between 9 and 20°C) than Δ_{47} thermometry (between 3 and 7°C). Though we acknowledge that these uncertainties are inherent to our study, it is likely that such higher variability on Th estimates might be observed in several other case

studies since likely resulting from two practical aspects of FIM measurements. First, FIM is focused on optical appreciation of phase transitions (between vapor, liquid states) that could induce a user-dependent bias on the measurements reproducibility. Second, the petrographic attribution of a FI population to a single fluid event is not easy. Hence, a misinterpretation between primary, pseudo-secondary or secondary FIs in carbonate minerals could lead to mixing between genetically different FI assemblages and consequently to a substantial bias on Th measurements. All these processes are inevitably propagated in the overall uncertainties on the trapping temperatures (Tt) and might contribute to the more scattered (and sometimes less accurate) temperature FI data than $T\Delta_{47}$ (as observed in the Paris basin). Importantly, we underline here that because of all these sources of cumulative uncertainties on FIM temperature data, the $\delta^{18}O_{water}$ values that were until recently commonly calculated from Th and $\delta^{18}O_{carb}$ might have been associated to relatively large uncertainties (that could be typically of several per mil), and could thus have led to misinterpretations in some cases (notably when FIs are rare or metastable and/or when paleo-pressure conditions are unknown and/or when FI's post entrapment re-equilibration are difficult to evaluate, particularly for soft minerals like calcite).

Finally, we emphasize here that in such context, coupling Δ_{47} and pressure-dependent FIM measurements may allow to evaluate paleo-pressure conditions of aqueous fluids precipitating carbonates. Indeed, a difference between the homogenization (Th) and the trapping (Tt) temperature is expected because of the pressure at trapping conditions and the compressibility of the fluid; with $Th+Pc=Tt=T\Delta_{47}$ (with $T\Delta_{47}$ and Th as known/measured values). Isochores that can be reconstructed from fluid inclusion measurements can then be associated with the independent $T\Delta_{47}$, so that both the temperature and pressure conditions during precipitation of the analyzed mineral can be reconstructed. Note that in the case of the Paris basin, paleopressures were too low to generate a significant and measureable offset between Th and Tt.

Case 2 (Fig. 9) considers partial or total resetting of FIM information as due to FI stretching or leakage by thermal reequilibration processes (e.g. overheating during further burial) in a carbonate mineral for which Δ_{47} primary composition is preserved. Here, FIM temperatures record the peak burial temperature of the FI host-rock (Tobin and Claxton, 2000) whereas the Δ_{47} signatures have still preserved the primary mineral growth temperature. All the samples of McDonalds et al. 2017 and some of Came et al. 2016 (c.f. D2 Aguthuna, D2 Catoch, D3 BoatHarbour) may reflect this configuration, as discussed by these authors. Such scenario records poly-phased thermal information of the host-rock (mineral growth and peak-burial temperatures), and preserves unbiased information on the fluid $\delta^{18}O_{water}$ (precisely calculated based on $T\Delta_{47}$) and salinity that governed mineral crystallization (assuming that no refill processes have occurred). Note that the calculation of paleopressure becomes here impossible as the thermal reequilibration process implies that FI have changed volume, density and liquid/vapor proportions (ie., $Th+Pc>Tt>T\Delta_{47}$).

Case 3 (Fig. 9) considers that Δ_{47} composition was partially or totally reset during burial via reordering of the isotopes distribution inside the carbonate lattice, whereas FIs retained their primary information ($T_h+Pc=Tt<T\Delta_{47}$). This scenario preserves the mineral growth temperature derived from FIs, whereas the Δ_{47} value reflects an apparent temperature. This apparent $T\Delta_{47}$ can represent any intermediate temperature between the crystallization temperature and the peak burial temperature or the present-day borehole temperature, depending on the degree (from partial to full) of isotopic redistribution/re-equilibration. Some

samples of Came et al. 2016 (c.f. D2BoatHarbour, D3Catoch) may reflect this configuration, as discussed by these authors.

In this case, it is thus recommended to use Th (preferably corrected for pressure) to calculate the $\delta^{18}O_{water}$ (as using $T\Delta_{47}$ for this calculation would be meaningless). In such unaltered FIs, with the assumption that no refill processes have occurred, the measured FI salinity can then be interpreted as the original salinity of the precipitating fluid. The calculations of paleopressure (Pc) is impossible.

Case 4 (Fig. 9) illustrates thermal alteration of both thermometers. It is likely that the two thermometers would not be affected in similar ways, because FI stretching or leakage are controlled by different parameters (Tobin and Claxton, 2000) than those governing ^{13}C-^{18}O bond reordering (e.g.; Henkes et al., 2014; Siman-Tov et al., 2016; Stolper and Eiler, 2015). No study to date have reported such configuration.

5. CONCLUSION

This study reports the first cross-consistent temperature estimates out of FIM and Δ_{47} measurements on both calcitic and dolomitic cements. This provides a rock-based validation of the inter-laboratory experimental Δ_{47}–T calibrations for calcite and dolomite recently published (Bonifacie et al. 2017), at least in the temperature range of 60-100°C. This also confirms that high-salinity fluids (from 0 to > 15 wt.% NaCl eq.) do not affect Δ_{47} signatures over crystallization of natural calcite and dolomite, as previously suggested for calcite based on laboratory experiments (Kluge and John 2015).

For the Middle Jurassic limestones of the Paris basin, the application of this methodology allows to constrain with high confidence the following characteristics for multiple diagenetic episodes that affected this formation (with Δ_{47} measurements allowing higher precision on precipitation temperature and $\delta^{18}O_{water}$ values, while significantly less time-consuming than FIM measurements, particularly for the Cal1 population for which FI were rare and metastable):

- **Cal1**: $T\Delta_{47}$ = 65±3°C ; T_{FIM} =70±11°C ; $\delta^{18}O_{water}$ = 3.1‰ ; Salinity = 14 wt.% NaCl eq.
- **Dol1:** $T\Delta_{47}$ = 98±7°C ; T_{FIM} =102±9°C ; $\delta^{18}O_{water}$ = 0.9‰ ; Salinity = 11.5 to 10.1 wt.% NaCl eq.
- **Cal2:** $T\Delta_{47}$ = 84±4°C ; T_{FIM} =88±15°C ; $\delta^{18}O_{water}$ = -3.4‰ ; Salinity = 12.8 to 0.2 wt.% NaCl eq.

More broadly, the combined application of FIM and Δ_{47} thermometry has the remarkable advantage to relieve the application of each proxy from its individual limitations, tied to either proxy conservativeness or working hypotheses. As such, this combined approach allows to access with an unprecedented level of confidence (in terms of both accuracy and precision) the paleofluid temperatures, salinity and oxygen isotopic composition. It can also, in some cases, reveal peak burial temperatures experienced by the host-rocks or the pressure at which carbonates precipitated. Importantly, we underline here that $\delta^{18}O_{water}$ values can now be determined with typical uncertainties of ~ ±1‰ when calculated from $T\Delta_{47}$ values. This contrasts to the several per mil uncertainties commonly reached when calculating $\delta^{18}O_{water}$ values via FIM temperature estimates often associated to several cumulative uncertainties resulting from strong working hypotheses (e.g., uncertainties on the paleo-pressure conditions and/or on the potential FI's post-entrapment re-equilibration, particularly for soft mineral like

calcites) or the characteristics of the FIs themselves (ie., rare and/or metastable).

Finally, joint application of FIM and Δ_{47} thermometry is highly recommended to interpret FI and Δ_{47} data in the most confident way as possible for the reconstruction of the paleo-temperature in sub-surface environments, and on samples that have been submitted to high temperature-time geological histories (for instance conditions sufficient to reach gas windows – 120/180°C).

6. ACKNOWLEGMENTS

We would like to thank Amandine Katz for help in the IPGP clumped isotope laboratory. We gratefully acknowledge Pascal Houel, Geneviève Bessereau, Benjamin Brigaud, Jean-Pierre Girard and Christophe Durlet for the constructive discussions about the geology, diagenesis and fluid-flow histories of the Paris basin. Michael Joachimski is thanked for tutoring the internship of Alina Götz at IFPEN. Marie-Christine Cacas is thanked for providing the financial support of her internship. The sub-surface cores of Baulne en Brie and Fossoy were available from the IFPEN storage collection of the BEPH (*Bureau Exploration-Production d'Hydrocarbures*). We are also grateful to Alain Buisson and Pierre André Duboin from Lundin Petroleum for sharing their knowledge on the petroleum reservoirs of the Paris basin. The paper benefitted from insightful reviews by Stephano Bernasconi and an anonymous reviewer.

FIGURES CAPTIONS:

Figure 1. Macrophotograph, microphotograph (CL and transmitted light) and thin section scan showing the major petrographic features of the investigated diagenetic cements. A, C) Cal1 consists of blocky crystals of non-ferroan calcite, displaying a very homogeneous bright orange CL pattern. Rock samples: BEBJ8 (1788,7m depth) and BEBJ12 (1785,3m depth), Baulne en Brie core interval. B) Cal2 consists of blocky crystals of non-ferroan calcite and displays a uniform dull red-to-brown CL pattern, with sectorial zoning. Rock sample: BEBJ2 (1792,8m depth), Baulne en Brie core interval. D) Dol 1 consists of not-luminescent saddle dolomite crsytals with distinctive curved crystal faces. Rock sample: FOS1610 (1610,3m depth), Fossoy core interval.

Figure 2. Schematic representation of the principle of Δ_{47} thermometry. Expected distribution of bonds between carbon and oxygen isotopes in calcite minerals precipitated from either cold or hot fluids (left and right cases, respectively). Carbonate ions CO_3^{2-} contain either clumped species, that is containing bonds between two heavy isotopes (ie., mostly $^{13}C^{18}O^{16}O_2$, but also $^{13}C^{17}O^{16}O_2$) colored in yellow, or not-clumped species colored in black (ie., mostly $^{12}C^{16}O_3$, but also $^{13}C^{16}O_3$, $^{12}C^{17}O^{18}O^{16}O$, etc). Ca^{2+} cations are colored in blue. The amount of clumped species is here exaggerated for the graphical representation.

Figure 3. Photomicrographs showing some petrographic features of the investigated FIs in the various mineral phases. A, C) Inclusion-rich saddle dolomite crystals (Dol1). B) Detail of FIs in Dol1, displaying variable shapes (e.g. crystallographically controlled, oblate or irregular) and consistent liquid/vapor ratio. D) Detail of two FIs with crystallographically controlled morphology and a liquid/vapor ratio of 0.90-0.95. E) Inclusion-rich Cal 1 crystals, that host two different FIA (in patch and along micro-fractures). F) Detail of a Cal1 crystal

where mono- and bi-phase FIs are densely distributed with shape controlled by crystallography.

Figure 4. Frequency histogram of homogenization temperatures (Th) in various mineral phases (orange for Cal1, red for Cal2 and grey for Dol1), compared with the Δ_{47} temperatures ($T\Delta_{47}$) measured in the same specimen (black bars). The Δ_{47} measurements were made on the same petrographic sub-zones where Th were measured. The width of the $T\Delta_{47}$ black bars are 1 S.E., their heights are arbitrary. A) and B) Cal1 blocky calcites samples BEBJ12 and BEBJ8, respectively). C) and D) Cal2 blocky calcites (samples BEBJ2 and BEBJ12, respectively). E) Dol1 saddle dolomite (sample FOS1610).

Figure 5. Trapping temperature (Tt) and pressure (Pt) calculation. A realistic geothermal gradient of 30°C/km in hydrostatic pressure conditions (10 MPa/km) has been used, together with surface temperatures of 20±5 °C

Figure 6. Transect of carbon ($\delta^{13}C_{carb}$) and oxygen ($\delta^{18}O_{carb}$) stable isotope compositions through a single Cal1 cement specimen of about 2 cm in length (sample BEBJ8). $\delta^{13}C_{carb}$ and $\delta^{18}O_{carb}$ values (reported in ‰ VPDB in red and black, respectively) are very homogeneous throughout the whole sample.

Figure 7. Precipitation temperatures obtained via Δ_{47} data ($T\Delta_{47}$) *versus* oxygen stable isotope compositions of carbonate ($\delta^{18}O_{carb}$). The color code is the same than in Figure 4. The five selected samples for the Δ_{47}-FIM inter-comparison are highlighted by bold squares. Reported uncertainties on Δ_{47} and $T\Delta_{47}$ are one standard error of the mean and are included in the symbol size for $\delta^{18}O_{carb}$. The long-term external reproducibility on Δ_{47} measurements obtained on more than 49 carbonate standards over the course of this study (ie., ± 0.018‰) is also reported on the upper right side for comparison. The average temperature calculated from all the samples of each of the three generations are also reported.

Figure 8. Comparison of temperature estimates derived from FIM and Δ_{47} measurements from this study and previous ones. Squares = data from the same cement specimens from this study (red and orange squares = calcites; grey square = dolomite). The dotted 1:1 line illustrate a configuration where $T\Delta_{47}$ = Th. Black circles = data from Came et al. (2016). Blue circles = data from MacDonald et al. (2017). Red circle = data from Millan et al. (2016). Th values were corrected for pressure effects in this study only (translucent squares). Uncertainties are reported as 1 S.E. for $T\Delta_{47}$ values for all studies and as 1 S.D. for Th data from all studies excepted for MacDonald et al. (2017) [for which uncertainties on Th data were not reported because of the large spread of Th data suggesting FIs reequilibration temperatures in each cement specimen].

Figure 9. Fate of FI and Δ_{47} thermometers in different hypothetical heating scenarios. This figure only describes cases for which neither dissolution/recrystallization nor petrographic changes of the host-crystals have occurred (e.g., no change of $\delta^{18}O$, $\delta^{13}C$ or elemental compositions since the time of precipitation) together with no change on fluid inclusion chemistry (assuming no refill). The notation Tt refers to the true FI trapping temperature, Th is the measured homogenization temperature, Pc is the pressure correction and $T\Delta_{47}$ is the temperature measured in the host-carbonate. Both $T\Delta_{47}$ and Tt can be either unaltered or (partially to fully) re-equilibrated since the time of the carbonate precipitation).

REFERENCES

Bakker, R.J., 2003. Package fluids 1 : Computer programs for analysis of fluid inclusion data and for modelling bulk fluid properties. Chem. Geol. 194, 3–23.

Bakker, R.J., 2009. Package fluids 3: correlations between equations of state, thermodynamics and fluid inclusions. Geofluids. 9, 63–74.

Bodnar, R, J. and Vityk, M, O., 1994. Interpretation of microthermometric data for H_2O-NaCl fluid inclusions. Fluid inclusions Miner. methods Appl. 18, 221-236

Bodnar, R., 1993. Revised equation and table for determining the freezing point depression of H_2O-NaCl solutions. Geochim. Cosmo. Acta. 57, 683–684.

Bonifacie, M., Calmels, D. and Eiler, J.M., 2013. Clumped isotope thermometry of marbles as an indicator of the closure temperatures of calcite and dolomite with respect to solid-state reordering of C – O bonds. Goldscmidt Conf. doi:10.1180/minmag.2013.077.5.2

Bonifacie, M., Calmels, D., Eiler, J.M., Horita, J., Chaduteau, C., Vasconcelos, C., Agrinier, P., Katz, A., Passey, B.H., Ferry, J.M. and Bourrand, J.J. 2017. Experimental calibration of the dolomite clumped isotope thermometer from 25 to 350°C, and implications for the temperature estimates for all (Ca, Mg, Fe) CO_3 carbonates digested at high temperature. Geochim. Cosmochim. Acta. 200, 255-279.

Brand, W.A., Assonov, S.S. and Coplen, T.B., 2010 Correction for the ^{17}O interference in $\delta^{13}C$ measurements when analyzing CO_2 with stable isotope mass spectrometry**.** Pure Appl. Chem., 82, 1719–1733.

Bristow, T.F., Bonifacie, M., Derkowski, A., Eiler, J.M. and Grotzinger, J.P., 2011. A hydrothermal origin for isotopically anomalous cap dolostone cements from south China. Nature 474, 68–71.

Came, R.E., Azmy, K., Tripati, A.K. and Olanipekun, B.-J., 2016. Comparison of clumped isotope signatures of dolomite cements to fluid inclusion thermometry in the temperature range of 73 to 176 °C. Geochim. Cosmochim. Acta. 199, 31-47.

Came, R.E., Eiler, J.M., Veizer, J., Azmy, K., Brand, U. and Weidman, C.R., 2007. Coupling of surface temperatures and atmospheric CO_2 concentrations during the Palaeozoic era. Nature 449, 198–201.

Dale, A., John, C.M., Mozley, P.S., Smalley, P.C. and Muggeridge, A.H., 2014. Time-capsule concretions: Unlocking burial diagenetic processes in the Mancos Shale using carbonate clumped isotopes. Earth Planet. Sci. Lett. 394, 30–37.

Defliese, W. and Lohmann, K., 2015. Non-linear mixing effects on mass-47 CO_2 clumped isotope thermometry: Patterns and implications. Rapid Commun. Mass. Spect. 81, 901–909. doi:10.1002/rcm.7175

Dennis, K.J., Affek, H.P., Passey, B.H., Schrag, D.P. and Eiler, J.M., 2011. Defining an absolute reference frame for 'clumped' isotope studies of CO_2. Geochim. Cosmochim. Acta 75, 7117–7131. doi:10.1016/j.gca.2011.09.025

Dennis, K.J. and Schrag, D.P., 2010. Clumped isotope thermometry of carbonatites as an indicator of diagenetic alteration. Geochim. Cosmochim. Acta 74, 4110–4122. doi:10.1016/j.gca.2010.04.005

Eiler, J.M., 2007. 'Clumped-isotope' geochemistry- The study of naturally-occurring, multiply-substituted isotopologues. Earth Planet. Sci. Lett. 262, 309–327. doi:10.1016/j.epsl.2007.08.020

Ferry, J.M., Passey, B.H., Vasconcelos, C. and Eiler, J.M., 2011. Formation of dolomite at 40-80°C in the Latemar carbonate buildup, Dolomites, Italy, from clumped isotope thermometry. Geology 39, 571–574. doi:10.1130/G31845.1

Gaulier, J.M. and Burrus, J., 1994. Modeling present and past thermal regimes in the Paris Basin - petroleum implications. Hydrocarb. Pet. Geol. 2, 61–75.

Ghosh, P., Adkins, J., Affek, H., Balta, B., Guo, W., Schauble, E.A., Schrag, D. and Eiler, J.M., 2006. $^{13}C–^{18}O$ bonds in carbonate minerals: a new kind of paleothermometer. Geochim. Cosmochim. Acta 70, 1439–1456.

Gleadow, A.J.W., Duddy, I.R., Green, P.F. and Lovering, J.F., 1986. Confined fission-track lengths in apatite - a diagnostic-tool for thermal history analysis. Contrib. to Mineral. Petrol. 94, 405–415.

Goldstein, R. and Reynolds, J., 1994. Systematics of Fluid Inclusions. SEPM Short Course Notes 31,188pp

Gonçalvès, J., Violette, S., Guillocheau, F., Robin, C., Pagel, M., Bruel, D., De Marsily, G. and Ledoux, E., 2004. Contribution of a three-dimensional regional scale basin model to the study of the past fluid flow evolution and the present hydrology of the Paris basin, France. Basin Res. 16, 569–586. doi:10.1111/j.1365-2117.2004.00243.x

Goncalves, J., Violette, S., Robin, C., Pagel, M., Guillocheau, F., de Marsily, G., Bruel, D. and Ledoux, E., 2003. 3-D modelling of salt and heat transport during the 248 My. evolution of the Paris Basin; diagenetic implications. Bull. la Soc. Geol. Fr. 174, 429–439.

Götze, J., 2012. Application of cathodoluminescence microscopy and spectroscopy in geosciences. Microsc. Microanal. 18, 1270–84. doi:10.1017/S1431927612001122

Green, P.F., Crowhurst, P. V, Duddy, I.R., 2004. Integration of AFTA and (U-Th)/He thermochronology to enhance the resolution and precision of thermal history reconstruction in the Anglesea-1 well, Otway Basin, SE Australia. PESA East. Australia. Basins Symp. II 15.

Gonçalvès, J., Pagel, M., Violette, S., Guillocheau, F. and Robin, C., 2010. Fluid inclusions as constraints in a three-dimensional hydro-thermo-mechanical model of the Paris basin, France. Basin Res. 22, 699–716.

Guilhaumou, N. and Gaulierc, J.M. 1991. Détermination de paléotempératures dans les roches-mères du bassin de Paris : Etude d'inclusions fluides et implications pour l'histoire thermique du bassin. Compte. R. Acad. Sci. Paris. 42, 773-780.

Henkes, G., Passey, B.H., Grossman, E.L., Shenton, B.J., Pérez-Huerta, A. and Yancey, T.E., 2014. Temperature limits for preservation of primary calcite clumped isotope paleotemperatures. Geochim. Cosmochim. Acta 139, 362–382. doi:10.1016/j.gca.2014.04.040

Henkes, G., Passey, B.H., Wanamaker, A.D., Grossman, E.L., Ambrose, W.G. and Carroll, M.L., 2013. Carbonate clumped isotope compositions of modern marine mollusk and brachiopod shells. Geochim. Cosmochim. Acta 106, 307–325. doi:10.1016/j.gca.2012.12.020

Hill, P.S., Tripati, A.K. and Schauble, E., 2014. Theoretical constraints on the effects of pH, salinity, and temperature on clumped isotope signatures of dissolved inorganic carbon species and precipitating carbonate minerals. Geochim. Cosmochim. Acta 125, 610–652. doi:10.1016/j.gca.2013.06.018

Horita, J., 2014. Oxygen and carbon isotope fractionation in the system dolomite–water–CO_2 to elevated temperatures. Geochim. Cosmochim. Acta 129, 111–124. doi:10.1016/j.gca.2013.12.027

Huntington, K.W. and Lechler, A.R., 2015. Carbonate clumped isotope thermometry in continental tectonics. Tectonophysics 647–648, 1–20. doi:10.1016/j.tecto.2015.02.019

Huntington, K.W., Wernicke, B.P. and Eiler, J.M., 2010. Influence of climate change and uplift on Colorado Plateau paleotemperatures from carbonate clumped isotope thermometry. Tectonics 29, 125-140. doi:10.1029/2009TC002449

Katz, A., Bonifacie, M., Hermoso, M. and Calmels, D., 2017. Laboratory-grown coccoliths exhibit no vital effect in clumped isotope composition on a range of geologically relevant temperatures. Geochim. Cosmochim. Acta in press. doi:http://dx.doi.org/10.1016

Kele, S., Breitenbach, S.F.M., Capezzuoli, E., Nele Meckler, A., Ziegler, M., Millan, I.M., Kluge, T., Deák, J., Hanselmann, K., John, C.M., Yan, H., Liu, Z. and Bernasconi, S.M., 2015. Temperature dependence of oxygen and clumped isotope fractionation in carbonates : a study of travertines and tufas in the 6-95°C temperature range, Geochim. Cosmochim. Acta 168, 172-192.

Kelson, J.R., Huntington, K.W., Schauer, A.J., Saenger, C., Lechler, A.R., 2017. Toward a universal carbonate clumped isotope calibration: Diverse synthesis and preparatory methods suggest a single temperature relationship. Geochim. Cosmochim. Acta 197, 104–131. doi:10.1016/j.gca.2016.10.010

Kluge, T. and John, C.M., 2015. Effects of brine chemistry and polymorphism on clumped isotopes revealed by laboratory precipitation of mono- and multiphase calcium carbonates. Geochim. Cosmochim. Acta 160, 155–168. doi:10.1016/j.gca.2015.03.031

Kluge, T., John, C.M., Jourdan, A.-L., Davis, S. and Crawshaw, J., 2015. Laboratory calibration of the calcium carbonate clumped isotope thermometer in the 25–250°C temperature range. Geochim. Cosmochim. Acta 157, 213–227. doi:10.1016/j.gca.2015.02.028

Krumgalz, B.S., Pogorelsky, R. and Pitzer, K.S., 1996. Volumetric properties of single aqueous electrolytes from zero to saturation concentration at 298.15 K represented by Pitzer's ion-interaction equations. J. Phys. Chem. 25, 639–663.

Loyd S. J., Corsetti F. A., Eagle R. A., Hagadorn J. W., Shen Y., Zhang X., Bonifacie M. and Tripati A. K. 2015. Evolution of neoproterozoic Wonoka-Shuram anomaly-aged carbonates: evidence from clumped isotope paleothermometry. Precambrian Res. 264, 179–191.

Lloyd, M.K., Eiler, J.M. and Nabelek, P.I., 2017. Clumped isotope thermometry of calcite and dolomite in a contact metamorphic environment. Geochim. Cosmochim. Acta 197, 323–344. doi:10.1016/j.gca.2016.10.037

Loyd, S.J., Corsetti, F., Eiler, J.M. and Tripati, A. K., 2012. Determining the Diagenetic Conditions of Concretion Formation: Assessing Temperatures and Pore Waters Using Clumped Isotopes. J. Sediment. Res. 82, 1006–1016. doi:10.2110/jsr.2012.85

Macdonald, J.M., Girard, J. and Larribau, A. E., 2017. Testing clumped isotopes as a reservoir characterisation tool: a comparison with fluid inclusions in a dolomitised sedimentary carbonate reservoir buried to 2-4 km. Geol. Soc. London submitted.

Machel, H.G., 1985. Cathodoluminescence in calcite and dolomite and its chemical interpretation. Geosciences Canada, 12, 139-147

Mangenot, X., Gasparrini, M., Rouchon, V. and Bonifacie, M. (in press). Basin scale thermal and fluid-flow histories revealed by carbonate clumped isotopes (Δ_{47}) - Middle Jurassic of the Paris Basin. Submitted to Sedimentology.

Matray, J.M., Lambert, M. and Fontes, J.C., 1994. Stable isotope conservation and origin of saline waters from the Middle Jurassic aquifer of the Paris Basin, France. Appl. Geochemistry 9, 297–309. doi:10.1016/0883-2927(94)90040-X

Mcneil, B. and Morris. E. 1992.The preparation of double-polished fluid inclusion wafers from friable, water-sensitive material. Mineralogical Magazine, 56 120-122.

Ménétrier, C., Élie, M., Martinez, L. and Le, A., 2005. Estimation of the maximum burial palaeotemperature for Toarcian and Callovo-Oxfordian samples in the central part of the Paris Basin using organic markers. Comptes Rendus Geosci. 337, 1323–1330.

Millán, M.I., Machel, H. and Bernasconi, S.M., 2016. Constraining temperatures of formation and composition of dolomitizing fluids in the upper devonian nisku formation (Alberta, Canada) with clumped isotopes. J. Sediment. Res. 86, 107–112. doi:10.2110/jsr.2016.6

Müller, I.A., Fernandez, A. Radke, J., Dijk, J.V., Bowen, D., Schwieters J. and Bernasconi, S.M., 2017. Carbonate clumped isotope analyses with the long-integration dual-inlet (LIDI) workflow: scratching at the lower sample weight boundaries. Rapid Commun. Mass Spectrom., 31, 1057–1066.

O'Neil J. R., Clayton R. N. and Mayeda T. K. (1969) Oxygen isotope fractionation in divalent metal carbonates. J. Chem. Phys. 51, 5547–5557.

Passey, B.H. and Henkes, G., 2012. Carbonate clumped isotope bond reordering and geospeedometry. Earth Planet. Sci. Lett. 223–236. doi:10.1016/j.epsl.2012.07.021

Roedder, E. and Bodnar, R. 1980. Geologic pressure determinations from fluid inclusion studies. Ann. Rev. Earth Planet 8, 263–301.

Rosenbaum, J. and Sheppard, S.M. 1986. An isotopic study of siderites, dolomites and ankerites at high temperatures. Geochim. Cosmochim. Acta, 50, 1147–1150. doi:10.1016/0016-7037(86)90396-0

Schauble, E., Ghosh, P. and Eiler, J.M., 2006. Preferential formation of ^{13}C–^{18}O bonds in carbonate minerals, estimated using first-principles lattice dynamics. Geochim. Cosmochim. Acta 70, 2510–2529. doi:10.1016/j.gca.2006.02.011

Sharp, Z.D. and Kirschner, D.L., 1994. Quartz-calcite oxygen isotope thermometry: A calibration based on natural isotopic variations. Geochim. Cosmochim. Acta 58, 4491–4501. doi:10.1016/0016-7037(94)90350-6

Shenton, B.J., Grossman, E.L., Passey, B.H., Henkes, G., Becker, T.P., Laya, J.C., Perez-Huerta, A., Becker, S.P. and Lawson, M., 2015. Clumped isotope thermometry in deeply buried sedimentary carbonates: The effects of bond reordering and recrystallization. Geol. Soc. Am. Bull. B31169.1. doi:10.1130/B31169.1

Siman-Tov, S., Affek, H.P., Matthews, A., Aharonov, E. and Reches, Z. 2016. Shear heating and clumped isotope reordering in carbonate faults. Earth Planet. Sci. Lett. 445, 136–145. doi:10.1016/j.epsl.2016.03.041

Stolper, D.A. and Eiler, J.M. 2015. The kinetics of solid-state isotope-exchange reactions for clumped isotopes: A study of inorganic calcites and apatites from natural and experimental samples. Am. J. Sci. 315, 363–411. doi:10.2475/05.2015.01

Tang, J., Dietzel, M., Fernandez, A., Tripati, A.K. and Rosenheim, B.E. 2014. Evaluation of kinetic effects on clumped isotope fractionation (Δ_{47}) during inorganic calcite precipitation. Geochim. Cosmochim. Acta 134, 120–136. doi:10.1016/j.gca.2014.03.005

Tobin, R.C. and Claxton, B.L. 2000. Multidisciplinary thermal maturity studies using vitrinite reflectance and fluid inclusion microthermometry: A new calibration of old techniques. Am. Assoc. Pet. Geol. Bull. 84, 1647–1665. doi:10.1306/8626BF29-173B-11D7-8645000102C1865D

Urey, H. C., Lowenstam, H. A., Epstein, S. and Mckinney, C. R. 1951. Measurement of paleotemperatures and temperatures of the Upper Cretaceous of England, Denmark, and the Southeastern United States. Geological Society of America Bulletin. 62, 399-416.

Vityk, M, O., Bodnar, R. and Schmidt, C. 1994. Fluid inclusions tectonothermobarometers : relation between pressure-temperature history and reequilibration morphology during crustal thickening. Geology, 22, 731–734.

Watkins, J.M. and Hunt, J.D. 2015. A process-based model for non-equilibrium clumped isotope effects in carbonates. Earth Planet. Sci. Lett. 432, 152–165. doi:10.1016/j.epsl.2015.09.042

Williams, S.H., Burden, E.T. and Mukhopadhyay, P.K., 1998. Thermal maturity and burial history of Paleozoic rocks in western Newfoundland. Can. J. Earth Sci. 35, 1307–1322. doi:10.1139/e98-045

Winkelstern, I.Z. and Lohmann, K.C. 2016. Shallow burial alteration of dolomite and limestone clumped isotope geochemistry. Geology 44, 467–470. doi:10.1130/G37809.1

Worden, R. H. and Matray, J. M., 1995. Cross formational flow in the Paris Basin. Basin Res. 7, 53–66.

Sample Name	Phase[(1)]	FI Occurence	Shape[(2)]	Size(3)	Filling degree (4)	**Homogeneization temp. (Th)**				**Ice melting temp. stable FI**		**Ice melting temp. metastable FI**		**Salinity**	
						Freq. Mode °C	Mean °C	STD °C	Range °C	Mode °C	Range °C	Mode °C	Range °C	Mode % wg. NaCl	Range % wg. NaCl
BEBJ8	Cal1	Isolated - in patch	CR, IR, RO	2-15	0.93/0.98	65/70	**62 (30)**	11	45-90 (30)	-11 (5)	-12.8/-10.1 (5)	-11.75 (14)	-15.3/-7.8 (14)	14 (5)	8.4/18.8 (5)
BEBJ12	Cal1	isolated	CR, IR	2-15	0.95/0.98	55/65	**64 (26)**	12	44-85 (26)	-	-	-	-	-	-
BEBJ2	Cal2	isolated or patch	CR, EG	2-10	0.90/0.98	75/85	**80 (32)**	10	60-100 (32)	-6 (11)	-9/-0.1 (11)	-7 (7)	-7/-3 (7)	Bimodale	0.2/12.8 (11)
BEBgeode	Cal2	In patch and along trail	CR, IR	-	0.90/0.98	75/80	**73 (31)**	20	60-95 (31)	-	-	-0.2 (3)	-0.4/1.2 (3)	-	-
FOS1610	Dol1	In patch (mineral core)	CR, IR	>5	0.90-0.96	90/95	**92 (31)**	9	70-110 (31)	-7.3 (9)	-6.7/-7.8 (9)	-	-	10.5 (9)	10.1/11.5 (9)

NOTES:
(1) Carbonate cement phases investigated: Cal1 and Cal2 from the Baulne en Brie core section and Dol1 from the Fossoy core
(2) The FIs shapes is distinguished as crystallographycally controlled (CR), irregular (IR), Elongated (EG)
(3) The inclusion size is given as length in µm
(4) F (degree of fill) stands for the volume fraction of the liquid phase at room temperature relative to the FI total volume

Table 1. Petrographic features of the main types of bi-phase FIs analyzed and microthermometric data, i.e. homogenization temperatures (Th), ice melting temperatures in stable (Tm_i) and metastable (Tm_{MET}) conditions. In parenthesis is reported the number of measurements accomplished for each of the three parameters. Salinities are expressed in wt. % NaCl eq. and were calculated, from stable Tm_i only, following the equation of Bodnar (1993).

Sample	Cement	CL character	n	$\delta^{18}O$	$\delta^{13}C$	$\Delta_{47CDES90}$ (1)	$\Delta_{47CDES25}$ (2)	1SE (3)	$T\Delta_{47}$ (4)	$\delta^{18}O_{water}$ (5)
				(‰, VPDB)	(‰, VPDB)	(‰, CDES)	(‰,CDES)	(‰)	°C	(‰, SMOW)
BAULNE EN BRIE CORE INTERVAL										
First generation of block calcite (Cal1 cements)										
BEBJ8 (X)	Cal1	Bright orange	3	-7.23±0.03	1.18±0.02	0.494±0.004	0.586	0.010	66±4	2.4
BEBJ6	Cal1	Bright orange	3	-5.62±0.14	2.04±0.07	0.500±0.024	0.592	0.014	63±6	3.6
BEBJ9	Cal1	Bright orange	2	-6.47±0.08	1.25±0.02	0.480±0.004	0.572	0.013	72±4	4.0
BEBJ11	Cal1	Bright orange	3	-6.06±0.04	1.78±0.03	0.496±0.006	0.588	0.010	65±6	3.4
BEBJ12(X)	Cal1	Bright orange	3	-5.84±0.05	1.65±0.02	0.504±0.010	0.596	0.010	61±4	3.0
BEBJ21	Cal1	Bright orange	2	-6.95±0.01	0.9±-0.01	0.501±0.025	0.593	0.018	62±8	2.2
BEBJ13	Cal1	Bright orange	2	-7.06±0.03	1.04±0.03	0.501±0.004	0.593	0.013	62±6	2.1
BEBJ5	Cal1	Bright orange	2	-5.86±0.04	1.66±0.01	0.493±0.018	0.585	0.013	66±7	3.7
BEBJ2 b	Cal1	Bright orange	2	-7.35±0.20	1.7±0.05	0.487±0.013	0.579	0.013	69±7	2.7
BEBJ2 c	Cal1	Bright orange	2	-5.69±0.06	1.45±0.07	0.500±0.011	0.592	0.013	63±6	3.5
CAL 1 -CEMENT POPULATION			***24***	***-6.41±0.68***	***1.45±0.36***	***0.496±0.007***	***0.588***	***0.004***	***65±3***	***3.1±0.7***
Second generation of block calcite (Cal2 cements)										
BEBJgeode (x)	Cal2	Dull red-brown	3	-15.26±0.06	1.99±0.17	0.459±0.011	0.551	0.010	83±6	-3.5
BEBJ2 (X)	Cal2	Dull red-brown	2	-15.15±0.01	1.79±0.18	0.456±0.001	0.548	0.013	84±6	-3.3
CAL 2 -CEMENT POPULATION			***5***	***-15.26±0.08***	***1.45±0.36***	***0.457±0.002***	***0.550***	***0.008***	***83±4***	***-3.4±0.1***
FOSSOY CORE INTERVAL										
First generation of saddle dolomite (DOL1)										
FOS1610 (x)	Dol1	not-luminescent	3	-9.57±0.05	1.76±0.03	0.432±0.008	0.524	0.010	**98±7**	**0.9**

Note.
(n) is the number of replicate measurements of the same carbonate powder, except for population averages (values in italic and bold font) for which the reported n is the total number of discrete analyses for the whole population.
(X) Selected samples for the comparison with FIM
(1) $\Delta_{47CDES90}$ are values relative to the 'carbon dioxide equilibrium scale' CDES and the 90°C acid digestion frames (ie., without acid fractionation correction). In this column, the reported uncertainties are one standard deviation for replicate measurements of the same carbonate powder.
(2) $\Delta_{47CDES25}$ are values relative to the 'carbon dioxide equilibrium scale' CDES, to which have been applied an acid fractionation factor of 0.092‰ (following Henkes et al. 2013) to transfer the $\Delta_{47CDES90}$ data into the 25°C acid digestion reference frame.
(3) S.E. = S.D / √n. When the standard deviation of the sample was lower than the long-term standard deviation of the homogeneous standards (average of ±0.018‰, n=49 in this study), SD of the standards were used to calculate SE for the samples.
(4) Paleotemperatures calculated using the inter-laboratory composite Δ_{47}-T calibration (Eq. 3 from Bonifacie et al. 2017)
(5) Oxygen isotope compositions of mineralizing waters calculated using TΔ_{47} and the equations of fractionation of oxygen isotopes between the carbonate and water of either O'Neil et al. (1969) for calcite and Horita (2014) for dolomite.

Table 2. Stable isotope Δ_{47}, $\delta^{18}O$ and $\delta^{13}C$ results from the diagenetic cements of Baulne en Brie and Fossoy core intervals.

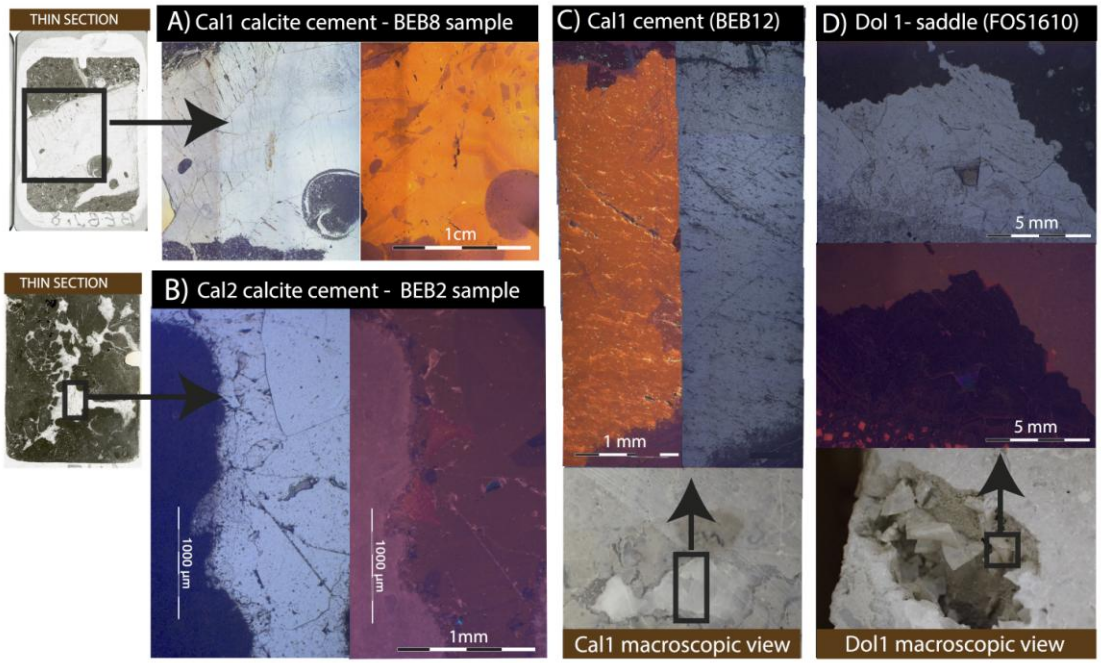

Fig. 1

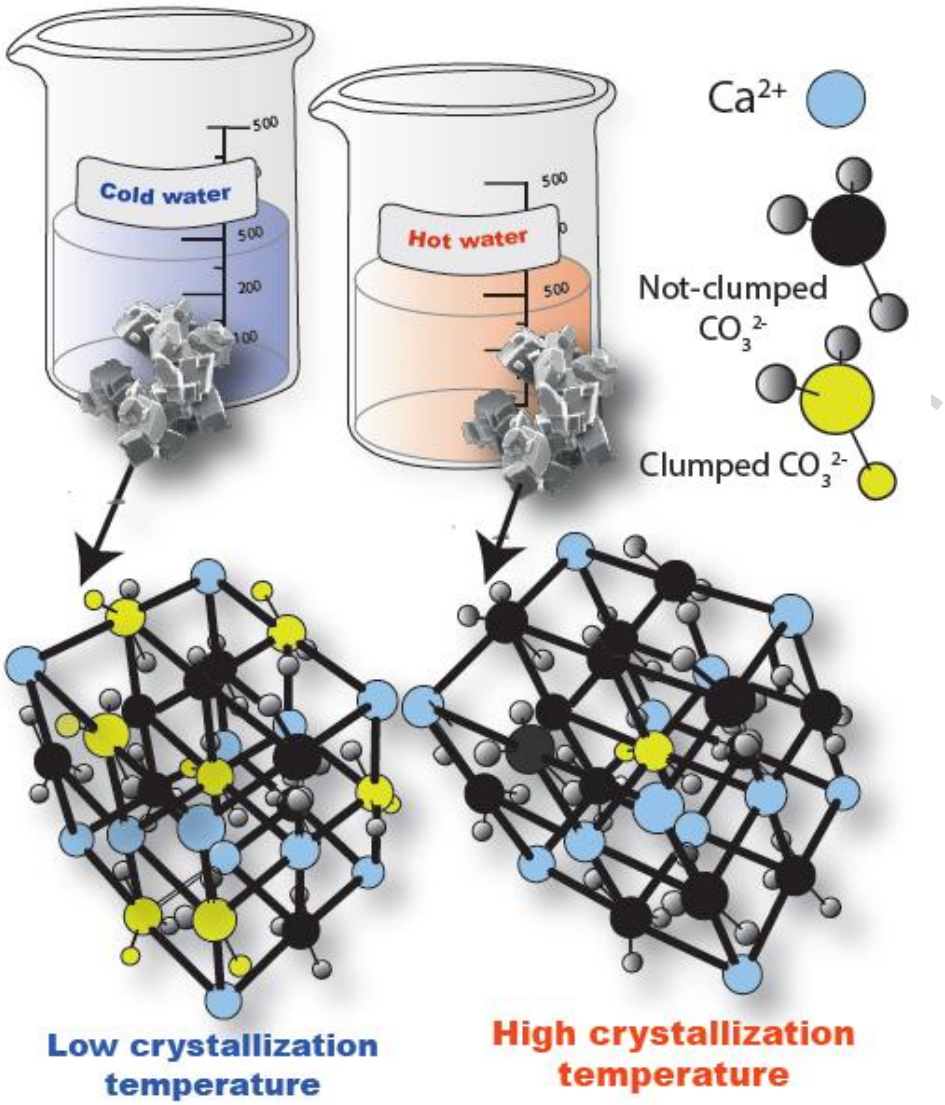

Fig. 2

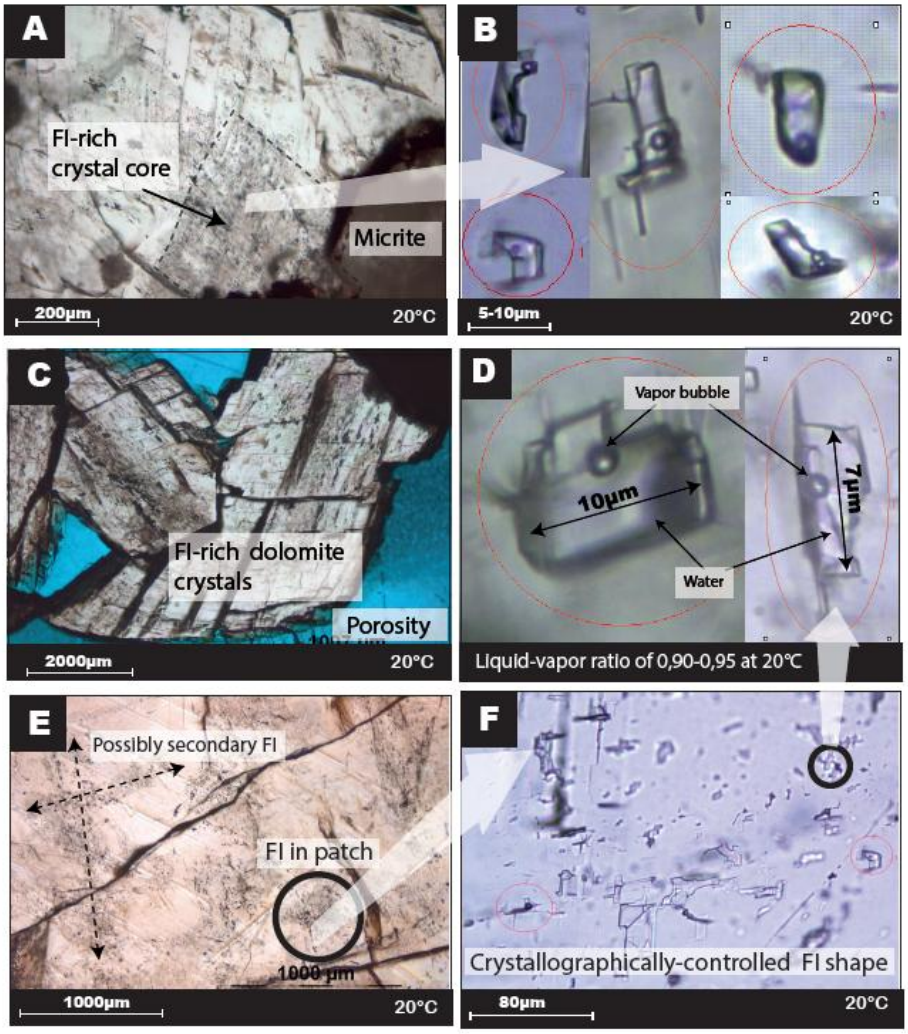

Fig. 3

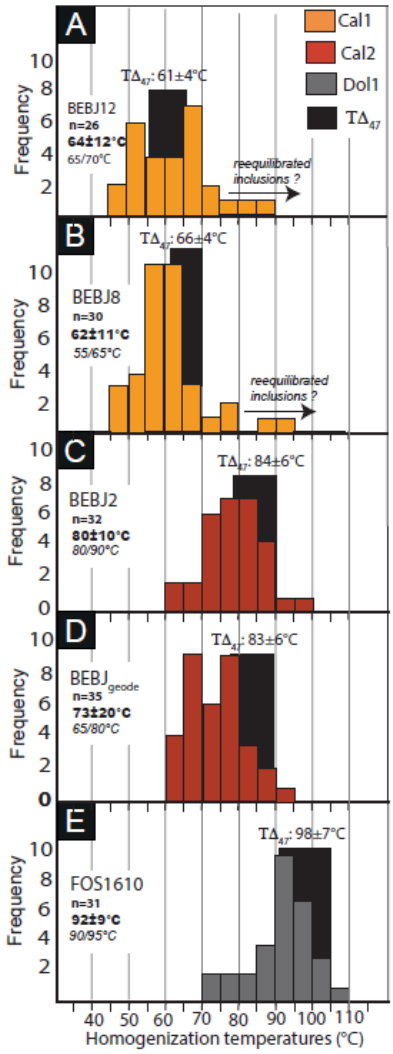

Fig. 4

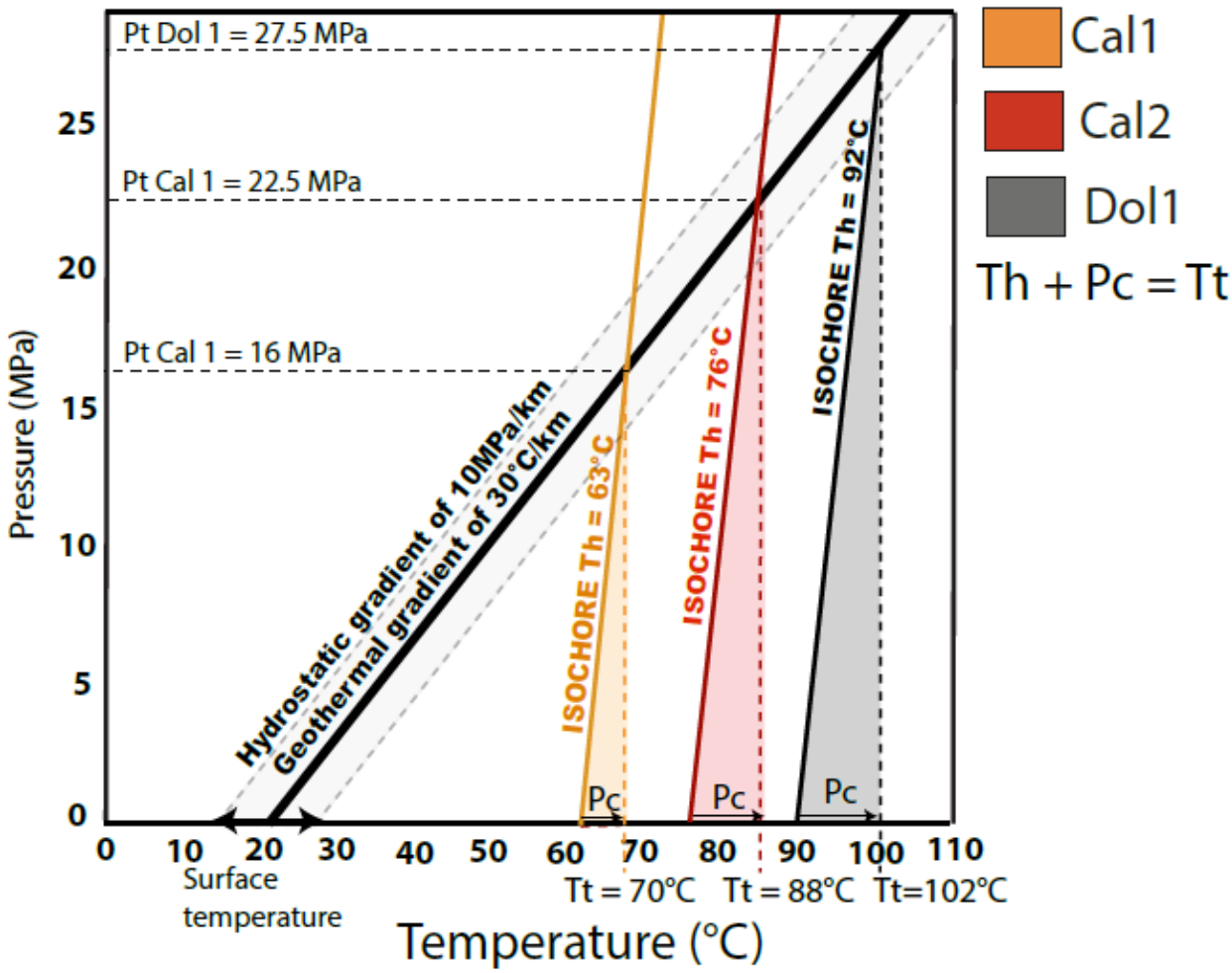

Fig. 5

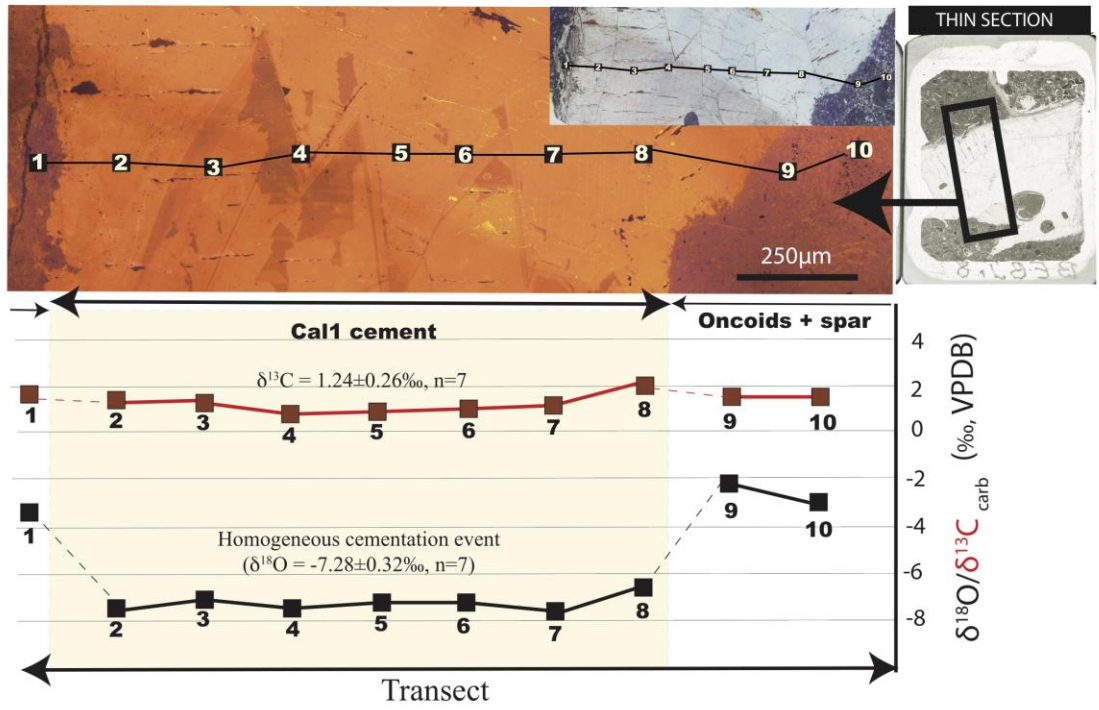

Fig. 6

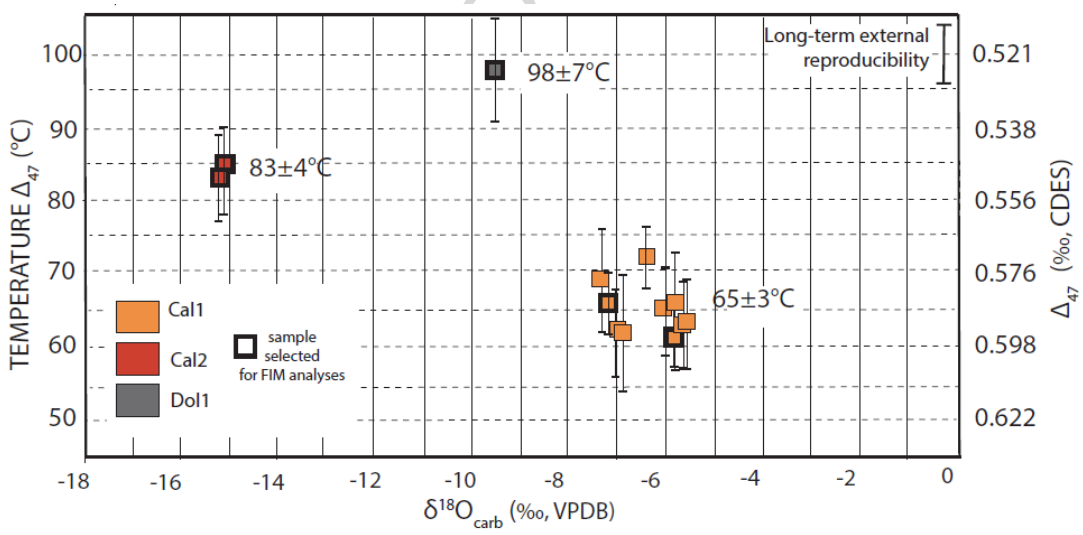

Fig. 7

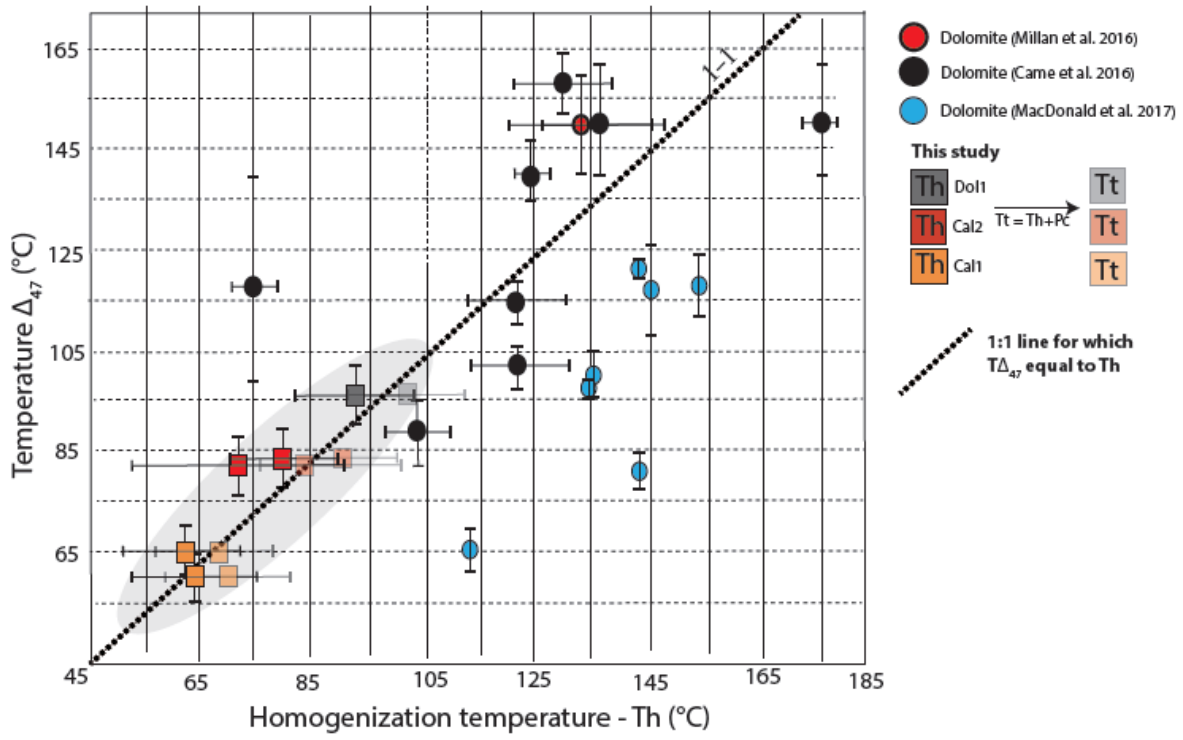
Temperature Δ47 (°C)
Homogenization temperature - Th (°C)
165
145
125
105
85
65
45
65
85
105
125
145
165
185
1:1
Dolomite (Millan et al. 2016)
Dolomite (Came et al. 2016)
Dolomite (MacDonald et al. 2017)
This study
Th Dol1
Th Cal2
Th Cal1
Tt = Th+Pc
Tt
Tt
Tt
1:1 line for which
TΔ47 equal to Th

Fig. 8

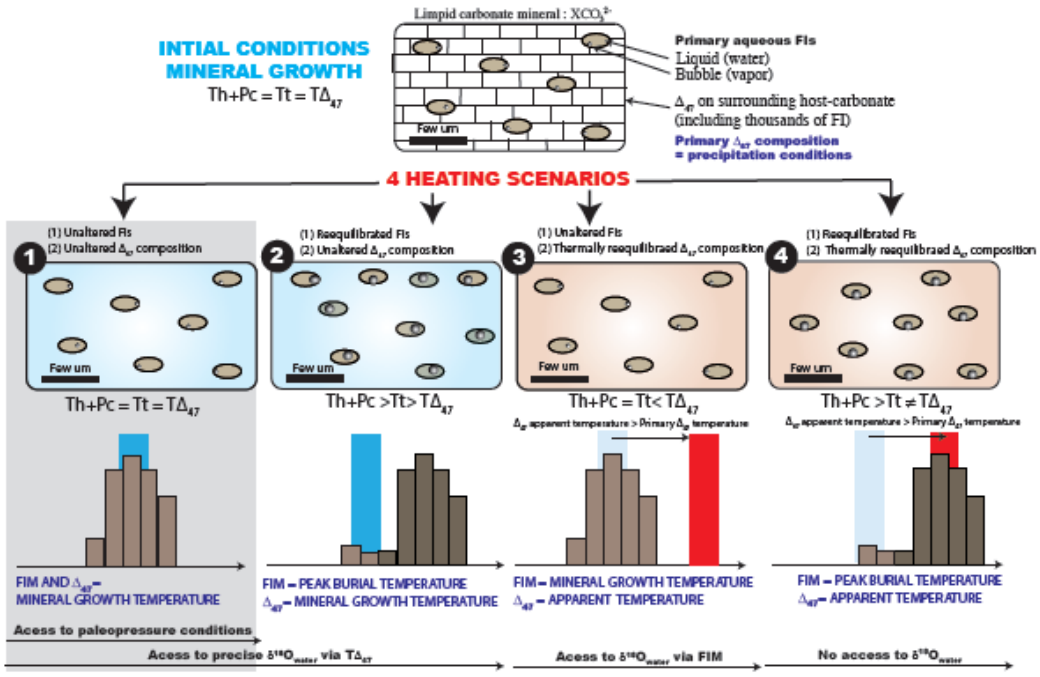
INTIAL CONDITIONS
MINERAL GROWTH
Th+Pc = Tt = TΔ47
Limpid carbonate mineral : XCO3 2-
Few um
Primary aqueous FIs
Liquid (water)
Bubble (vapor)
Δ47 on surrounding host-carbonate
(including thousands of FI)
Primary Δ47 composition
= precipitation conditions
4 HEATING SCENARIOS
1
(1) Unaltered FIs
(2) Unaltered Δ47 composition
Th+Pc = Tt = TΔ47
FIM AND Δ47 =
MINERAL GROWTH TEMPERATURE
Acess to paleopressure conditions
Access to precise δ18Owater via TΔ47
2
(1) Reequilibrated FIs
(2) Unaltered Δ47 composition
Th+Pc >Tt> TΔ47
FIM = PEAK BURIAL TEMPERATURE
Δ47 = MINERAL GROWTH TEMPERATURE
3
(1) Unaltered FIs
(2) Thermally reequilibraed Δ47 composition
Th+Pc = Tt< TΔ47
FIM = MINERAL GROWTH TEMPERATURE
Δ47 = APPARENT TEMPERATURE
Acess to δ18Owater via FIM
4
(1) Reequilibrated FIs
(2) Thermally reequilibraed Δ47 composition
Th+Pc >Tt ≠ TΔ47
FIM = PEAK BURIAL TEMPERATURE
Δ47 = APPARENT TEMPERATURE
No access to δ18Owater

Fig. 9

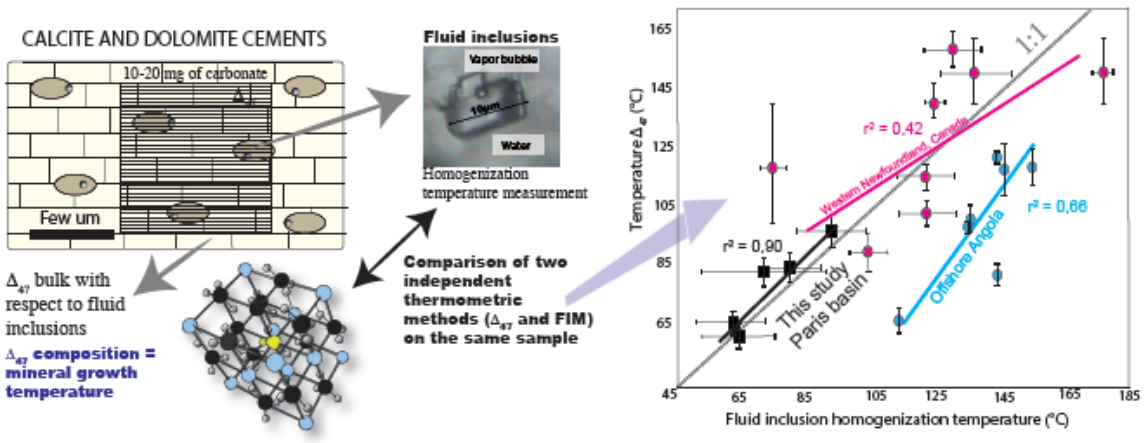

Graphical abstract